Low Moisture Extrusion of Intermediate Wheatgrass-pea Starch Blends: Production and Characterization of Ready-to-eat Extruded Snacks

Hazrat Usman
University of Minnesota
Cecia Flores-Sanchez
University of Minnesota
George Amponsah Annor
gannor@umn.edu
University of Minnesota

Research Article

Keywords: perennial grains, sustainable agriculture, optimization, extrusion, thermal processing

Posted Date: February 2nd, 2026

DOI: https://doi.org/10.21203/rs.3.rs-8713961/v1

Additional Declarations: No competing interests reported.

LOW MOISTURE EXTRUSION OF INTERMEDIATE WHEATGRASS-PEA STARCH BLENDS: PRODUCTION AND CHARACTERIZATION OF READY-TO-EAT EXTRUDED SNACKS

Hazrat Usman, Cecia Flores-Sanchez, and George Amponsah Annor*
Department of Food Science and Nutrition,
University of Minnesota,
1334 Eckles Avenue,
Saint Paul, MN 55108, USA.

* Correspondence:
George Amponsah Annor
gannor@umn.edu

Abstract

Intermediate wheatgrass (*Thinopyrum intermedium*, IWG), enriched with protein and dietary fiber, has the potential to deliver both food and ecosystem service benefits. However, its lower starch content limits expansion of the extrudates during extrusion, reducing its suitability for ready-to-eat (RTE) snacks. Pea starch, a by-product in pea protein production, can enhance functional attributes of extruded products. Therefore, this systematic study was conducted to optimize the extrusion parameters to produce RTE snacks through a co-rotating twin screw extruder to meet the increasing demand for nutritious novel foods. Box-Behnken design coupled with response surface methodology was used to investigate the effects of pea starch percentage, feed moisture, screw speed and barrel temperature on product responses (expansion ratio, bulk density, hardness, crispiness, color (L*), water absorption index, water solubility index) and processing response (specific mechanical energy) whose value varied from 1.08 to 2.16, 0.13 to 0.34 g/cm^3, 30.33 to 109.74 (N), 284.68 to 751.43 N.s, 72.71 to 80.55, 4.49 to 6.59 g/g, 21.45 to 35.91% and 586.40 to1132.09 KJ/Kg respectively. Response surface regression models were established to determine the response variables. Regression models for all the responses were highly significant ($p < 0.01$) with co-efficient determination ranged from 0.80 to 0.98. The optimum conditions obtained by multi-response optimization for the development of RTE extruded snacks were IWG flour to pea starch ratio (46:54), feed moisture 19.57%, screw speed 241 rpm and barrel temperature 131°C. This paper therefore explores the optimization of processing conditions for the development of RTE extruded snacks from IWG-pea starch blends.

Key words: perennial grains, sustainable agriculture, optimization, extrusion, thermal processing

1. Introduction

Worldwide, the majority of cropland is occupied by annual crops, which provide approximately 50% of global caloric intake, but are associated with several environmental problems, including water pollution, soil erosion, and loss of animal habitats (Kearney, 2010; Monfreda et al., 2008). An important strategy to lessen these environmental impacts is the development of perennial crops (Glover et al., 2010). Because of their extensive and deep root systems, which improve resilience to water scarcity by reaching the underground stored water. Perennial crops also support sustainable agroecosystems by minimizing soil erosion, cycling nutrients , and sequestering carbon through continuous deep roots activity (Clément et al., 2022; Förster et al., 2025)

A significant advancement in sustainable agriculture is achieved through the development of Intermediate wheatgrass (*Thinopyrum intermedium*, IWG), commercially known as Kernza® by the Land Institute in Kansas (USA). It is the first perennial grain crop commercialized in the US to provide both forage and gain (Ginot et al., 2024; Law et al., 2022). Like wheat, rye, and barley, IWG is a member of the Triticeae tribe within the Poaceae grass family and related to wheat (Boakye, Okyere, Bharathi, et al., 2023; Cetiner et al., 2023). In 1932, IWG was introduced from the Russian region of Miakop for the control of soil erosion and forage. IWG gained attention for its high biomass yield and tolerance to frost and drought. Its agronomic adaptability supports dual use systems, offering grains and straw harvest in summer, as well as spring and fall forage through regrowth (Rusch et al., 2025; Favre et al., 2019). This dual system may offer potential for diversifying farmers' income, but its overall productivity and profitability remain under evaluation (Clément et al., 2022). In the 1980s, efforts began to domesticate IWG for grain production, with significant breeding advancements made over the past two decades (DeHaan et al., 2018). A major milestone was achieved in 2020 when the University of Minnesota released the first grain producing IWG cultivar (Bajgain et al., 2020). Although globally, most the food and feed is supplied by annual grains, currently across North America and Europe several breeding programs are working on the enhancement of IWG's viability as a commercial grain crop contributing to develop perennial grains that support both food security and ecosystem services such as carbon sequestration, nitrate leaching reduction, and erosion control (Crain et al., 2020).

In addition to ecological advantages, IWG exhibits nutritional and functional properties. It contains higher protein (50%), dietary fiber (129%), ash (65%), calcium (267%), and selenium (492%), along with elevated riboflavin and folate, though niacin is lower as compared to traditional whole wheat flour (Craine & DeHaan, 2024; Schendel et al., 2015). Functionally, IWG starch and dough properties resemble those of wheat. Rheological analysis revealed that IWG protein forms a gas holding network, supporting its potential in breadmaking (Grandal et al., 2025). IWG has been explored for the food application (Boakye, Okyere, & Annor, 2023).

Starch plays a key role in extrudate expansion through its gelatinization, with higher starch content typically resulting in improved expansion ratios (Van Hoan et al., 2010). IWG has more protein and lower starch content which results less expansion of the extrudates (Tyl & Ismail, 2019; Boakye et al., 2022). In our research, we incorporated different levels of pea starch into IWG whole flour to get more expansion of the extrudates.

Incorporating legumes like pea (*Pisum sativum*) as a key ingredient in the formulation of snacks food can enhance the nutritional value by increasing protein and fiber content. Pea-based expanded snacks have been developed using different combinations of pea flour, fiber, and starch, along with varied extrusion temperatures. Pea starch with other ingredients in combination can further enhance the sensory attributes of the snacks (Maskus & Arntfield, 2015; LUO, 2019). In response to increasing consumer interest in plant-based proteins because of their high nutritional value and affordability, the food industry scales up pea protein concentrates and isolates production, with a market of 34.8 million USD in 2020. Consequently, significant amounts of pea starch are produced as a by-product, highlighting the need for value-added applications of pea starch (Rangira et al., 2020).

Pea starch makes up about 44.7% to 50.3% of whole pea flour and is composed of two polysaccharides: amylose and amylopectin (Rangira et al., 2020). The high amount of amylose in pulse starch imparts exceptional functional properties including high gelatinization temperature, rapid retrogradation, resistance to shear thinning and strong gel elasticity. These properties make it ideal for products like starch noodles commonly made by extruding dough formed from native and pregelatinized starch (N. Wang et al., 2014). Pea starch can be a viable alternative to traditional starch sources like wheat in animal feed, especially for pigs (Thingnes et al., 2013).

Snacks are common commonly referred to small portions of food eaten between meals, with definitions varying by timing, quantity, or type (Ali et al., 2024). Extruded snacks, such as puffed ready-to-eat (RTE) cereals, have gained widespread popularity globally, particularly among children (Bhat et al., 2019; *Annex 6 - Glossary | Food Standards Agency*, 2023). In most snack products, formulations are cereals like wheat, corn, and rice, with some portion of oats, potatoes, and other ingredients are typically used (Nor et al., 2013; Sharma & Gujral, 2013).

RTE snacks have become essential to many individuals, and the demand for these snacks are growing as the consumers desired convenience, texture appealing, and healthy products (Chadha et al., 2021; Brennan et al., 2013). The global market for extruded snacks remains strong, valued at USD 71.5 billion in 2024 and is forecasted to reach USD 104.8 billion by 2030, growing at a CAGR of 6.6% (Brennan et al., 2013; ltd, 2025).

Extrusion technology is widely used in producing cereal based RTE snacks due to its ease of operation and ability to create diverse, appealing textures and shapes (Brennan et al., 2013)

During extrusion processing, parameters like barrel temperature, moisture of the feed, materials composition, screw speed and its configuration effect the quality of extrudates (Brennan et al., 2013). Twin-screw extrusion (TSE) is preferred in food industry due its automated control, energy efficiency, cost-effectiveness high capacity, continuous operations and for its flexibility in adjusting screw profile, barrel temperature, and rotational speed tailored specific formulations (Dey et al., 2024; J. Wang et al., 2019).

Extrusion technology is widely used to manufacture several food products like pasta, noodles snacks, breakfast cereals, baby food, meat analogues, pet foods, texturized vegetables proteins and more (Ali et al., 2024; Boakye, Okyere, & Annor, 2023; Geetha et al., 2014; N. Wang et al., 2012). Extrusion is a high-temperature and a short-time process that involves the flow of one or more polymer melts and the integration of multiple operations such as mixing, kneading, shearing and cooking the raw materials. The mixed ingredients are forced through a die of specific size and shape, then cut into a range of food products (Bordoloi & Ganguly, 2014). The expansion and crispness achieved through temperature and pressure differentials (Brennan et al., 2013). Extrusion cooking is a multi-step, multi-functional and thermal/mechanical process that affects nutritional quality, degrades some components, it also offers benefits such as starch gelatinization, destruction of anti-nutritional factors, increased soluble fiber, and reduced lipid oxidation (S. Singh et al., 2007; Choton et al., 2020). However, it may also reduce levels of resistant and slowly digestible starch (Boakye, Okyere, & Annor, 2023).

Low moisture (below 30%) extrusion is widely used in the production of expanded snacks (Beck et al., 2017). The expansion of extrudates, primarily driven by starch transformation, enhances the crispiness of products and attracts consumers (Brennan et al., 2013). As a result, extrusion cooking has become an extensively accepted industrial technology across food and feed sectors, with market demand projected to reach USD 99.7 billion by 2026 (Dey et al., 2024; *Food Extrusion Market*, 2015).

The objective of our research was to produce expanded ready-to-eat snacks using whole-grain flour from intermediate wheatgrass blended with various levels of pea starch. Response surface methodology (RSM) was employed to evaluate the physical and functional properties of IWG-pea starch blends extrudates and optimize processing conditions to scale up the extrusion parameters.

2. MATERIALS AND METHODS

2.1 Materials

Intermediate wheatgrass (IWG) grains known as Kernza® variety MN Clearwater were supplied by Perennial Pantry, SBC (12651 Zenith Ave. S, Ste. 107, Burnsville, MN 55337). The grains were stored at 4 °C to preserve quality. Milling was conducted using a hammer mill equipped with sieve number 40 (sieve size ~ 0.5 mm) in the Department of Food Science and Nutrition at the University of Minnesota. The grains were ground into whole flour, which included all components of the kernel. The IWG whole flour was blended with different levels of pea starch and used for extrudate production.

Pea starch (Item No. PS85-B), preferred for extrusion applications, was obtained from PURIS (811 Glenwood Ave, Suite 110, Minneapolis, MN 55405, USA). It was used as a key ingredient in formulating blends (30%, 50% and 70%) with IWG-flour for extrusion processing. A twin shell dry blender (The Patterson-Kelley Co., Inc. East Stroudsburg, Pennsylvania) was used to thoroughly mix the IWG-pea starch blends for 10 minutes to get uniform mixture.

2.2 Experimental design

A Box-Behnken design, coupled with response surface methodology (RSM) was developed by Design-Expert: STAT-EASE 360®. The factors included pea starch percentage as X_1, feed moisture percentage, as X_2, screw speed as X_3 and barrel temperature °C as X_4. The lowest, highest and mid values of the variables were coded as −1 and +1, respectively, and the mid value coded as 0 see **Table 1**.

The experimental ranges were determined through preliminary trials performed following the factors' ranges applied by Boakye et al., (2022) to ensure continuous, safe and effective extrusion operation. Pea starch below 30% had negligible impacts on the extrudates, while above 70% could hinder the effect and properties of the main ingredient, IWG whole flour, in the final products. Feed moisture below 19% created high load (torque) and excessive pressure in extruders, which led the machine to stop, whereas above 23% feed moisture prevented product expansion. Screw speeds less than 200 rpm and above 300 rpm resulted undesirable products. Barrel temperatures below 120 °C provided uncooked, hard and undesirable exudates, while those above 150 °C led to material burning. The results of Boakye et al., (2022) revealed that 28% moisture, 400 rpm, and 170 °C, expansion was minimal (expansion ratio = 0.97 ± 0.01). A Box-Behnken design coupled with response surface methodology (27 variable combinations with three center points) was applied to evaluate the interactive effects of pea starch content, feed moisture, screw speed, and barrel temperature at a constant feed rate of 2.5 kg/hour on product functional properties as shown in **Table 3**.

2.3 Extrusion of IWG-Pea starch blends

A co-rotating twin-screw (Brabender R © TwinLab-F20/40) extruder with an 800 mm screw length and 20 mm diameter (resulting in an L/D ratio of 40:1) was used for extruding of IWG flour-pea starch blends extrusion. The extruder comprised of six heating zones, which were controlled independently. The first three heating zones of the extruder were set at 50°C, 80°C, and 120°C. In comparison, the last three zones varied according to the experimental design (**Table 2**). Screw speed ranging (200rpm to 300 rpm) was regulated according to the experimental design (**Table 3**). The screw was designed in such a way that the first section contained conveying elements, with the next containing both conveying and kneading elements. Finally, the high shear section contained conveying, reverse conveying, and kneading elements as represented in **Figure 1**. Desired moisture (19%, 21% and 23%) of the feed was achieved by injecting calculated amounts of water directly into the barrel using a peristaltic pump. A constant feed rate of 2.5kg/h was maintained through the experiment. A 5mm circular die was fitted at the exit of the extruder to shape the extrudates. After extrusion, extruded samples were dried at 50 °C for 18 hours, packed in airtight zip-lock bags and subsequently stored under refrigerated conditions (~4 °C) until further analysis.

2.4 Expansion ratio

A digital Vernier caliper (Toolshop®, Menard Inc., Eau Claire, WI, USA) was used to precisely measure the diameter of the ten randomly selected exudates from each experimental run. The expansion ratio was then calculated by dividing the cross-sectional diameter of the extrudates by the diameter of the circular die, following the method as described by (Boakye et al., 2022).

$$\text{Expansion ratio} = \frac{Average\ diameter\ of\ the\ extruadates\ (mm)}{Average\ diameter\ of\ the\ die\ (mm)} \quad \ldots\ldots\ldots\ldots\ldots\ldots\ldots\ldots\ldots\ldots\ (1)$$

2.5 Bulk density

The glass beads displacement method described by Rangira et al., (2020), with some modification was used to determine the bulk density of the extrudates. Bulk density was calculated by dividing the mass of the extrudates by the recorded displaced volume.

$$\text{Bulk density} = \frac{Mass\ of\ the\ extruadates\ (g)}{Volume\ of\ the\ displaced\ rape\ seeds\ by\ extrudates\ (cm3)} \quad \ldots\ldots\ldots\ldots\ldots\ldots\ldots\ldots\ (2)$$

2.6 Water absorption index (WAI) and Water solubility index (WSI)

Water absorption index and Water solubility index were determined according to the method described by (Boakye et al., 2022). UDY cyclone sample mill (Udy Corp., Fort Collins, CO, USA) equipped with a 0.5 mm screen was used to mill the dried extruded samples. For each analysis, two grams of powdered sample were thoroughly mixed with 20 ml of distilled water using a vortex and agitated for 30 minutes at room temperature using G24 environmental incubator shaker (New Brunswick Scientific Co., Inc. Edison N.J. U.S.A.) to ensure uniform hydration. The mixture was then centrifuged at 3000 g for 10 minutes to separate the soluble and insoluble fractions. The resulting supernatant was carefully collected in pre-weighted aluminum pans and dried at 135°C for 2 hours to determine the dry solids. WAI was calculated by determining the weight of the hydrated sediment residue remaining after centrifugation, while WSI was expressed as the percentage of dried solids in the supernatant relative to the original sample weight. This approach enables the assessment of the swelling capacity and solubility behavior of the samples under aqueous conditions.

$$\text{Water absorption index (g/g)} = \frac{Weight\ gain\ bygel(g)}{Dry\ weight\ of\ extrudate\ sample\ (g)} \quad \ldots\ldots\ldots\ldots\ldots\ldots\ldots\ldots\ldots\ (3)$$

$$\text{Water solubility index (\%)} = \frac{Weight\ of\ dissolved\ solids\ in\ supernatant}{Weight\ of\ dry\ solids} \times 100 \quad \ldots\ldots\ldots\ldots\ldots\ldots\ldots.\ (4)$$

2.7 Hardness and Crispiness

The hardness of the extrudates was assessed using a TA.XT Plus Texture Analyzer, as described by (Boakye et al., 2022), with slight modifications to the testing parameters. A 13 mm cylindrical probe was employed to perform a compression test under controlled conditions. The analysis was conducted with a 2 mm/s pretest speed, followed by both test and post-test speeds set at 0.4 mm/s, 50% strain, 5-second hold time, and a 5 g trigger force. The instrument's Exponent software was used to record the force hardness values in Newtons and crispiness values in Newton. Second.

2.8 Color

A Chroma Meter (CR-200; Minolta, Tokyo, Japan) was used to determine the color of milled extrudates with a method reported by (Zhang et al., 2020). Three color parameters (L*, a* and b*) were noted. These parameters indicate: L* (ranging from 0 = black to 100 = white), a* (positive values indicating red and negative indicating green), and b* (positive values indicating yellow and negative indicating blue).

2.9 Specific Mechanical Energy (SME)

The specific mechanical energy was calculated torque percentage given by the extruder software using the data of the power consumed per unit of time and the total feed input (solids + water) (Heredia-Olea et al., 2020). During extrusion, real time data such as zone temperature, motor torque, and pressure were continuously recorded using a data acquisition system coupled with the Brabender® extruder. One data point was collected per second, and average values for pressure and torque were derived from 20 randomly selected readings under steady state conditions (Boakye et al., 2023). Specific mechanical energy (SME, kJ/kg) was calculated from screw speed, measured torque and power as described by (Kristiawan et al., 2018).

$$SME = \frac{\frac{N}{Nmax} \times \tau - \tau empty/100}{Q} \times Pmax \times 3600 \quad \ldots\ldots (5)$$

Where N and N_{max} represent the actual and maximum screw speeds, while τ and τ_{empty} denote the measured torque under loaded and no-load conditions respectively. The maximum power of the extruder is Pmax and Q is the feed flow rate (kg/h).

2.10 Statistical analysis

A Box-Behnken design coupled with response surface methodology (**Table 3**) was applied to evaluate the interactive effects of four factors (pea starch content, feed moisture, screw speed and barrel temperature) at a constant feed rate of 2.5 kg/hour on product functional properties. Design-Expert:STAT-EASE 360® was used for data analysis, and graphical presentation. JMP software student version 18 was used for graphical presentation of the optimized data. The effects of process conditions on product responses and process response were evaluated. The experimental data obtained was fitted into quadratic equations, as shown in equation 6.

$$Y = A_0 + A_1X_1 + A_2X_2 + A_3X_3 + A_4X_4 + A_{12}X_1X_2 + A_{13}X_1X_3 + A_{14}X_1X_4 + A_{23}X_2X_3 + A_{24}X_2X_4 + A_{34}X_3X_4 + A_{11}X_1^2 + A_{22}X_2^2 + A_{33}X_3^2 + A_{44}X_4^2 \quad \ldots\ldots (6)$$

Where Y denotes the predicted responses (ER, BD, WAI, WSI, Hardness, Crispiness, SME and Color), A_o is the interception, A_1 to A_4 are the coefficients of the linear terms, A_{12} to A_{34} represent the coefficients of two-way interaction terms, A_{11} to A_{44} correspond to the coefficients of the quadratic terms. The coded variables X_1, X_2, X_3, and X_4 represent the levels of pea starch, feed moisture, screw speed, and temperature, respectively.

Analysis of variance (ANOVA) was conducted using Design-Expert: STAT-EASE 360® to evaluate model fitness and the significance of response coefficients at a 95% confidence level. Correlation analysis among response variables was performed.

2.11 Optimization

After optimizing each individual response numerically, corresponding criteria for both the responses and the independent variables were established to conduct the multi-response optimization using Design-Expert: STAT-EASE 360®.

3. RESULTS AND DISCUSSION

3.1 RSM

Response Surface Methodology (RSM), a statistical technique that describes the relationship between process variables and product characteristics was used in this study due to its ability to generate accurate and reproducible second-order models with a minimal number of experimental runs. It is commonly applied to plan a response surface within a specified region of interest, optimize responses, or determine operating conditions that meet target specifications. For each response variable, second-order polynomial regression models were developed to fit the experimental data using Design-Expert:STAT-EASE 360®. The experimental results for measured responses are summarized in **Table 4**. All developed models were statistically significant ($p < 0.05$), while the lack-of-fit tests were not significant ($p > 0.05$), indicating that the models adequately represented the experimental data. Analysis of variance (ANOVA) was conducted to evaluate the significance of individual model terms as represented in **Table 5**. The coefficient of determination (R^2), and adjusted R^2 values, predicted R^2 followed by adequate precision values for each response variable are shown in **Table 4**. The R^2 values ranging from 0.80 to 0.98 for all responses, indicating strong model reliability. Furthermore, adequate precision of each response model which measures the signal to noise ratio and reflects the adequacy of the model in distinguishing meaningful variation from background noise, was calculated to be than 4 which is generally considered acceptable, and this value indicates that the model possesses a sufficiently strong signal (**Table 6**). Consequently, the model is deemed suitable for exploring and optimizing within the defined design space. To facilitate interpretation, three-dimensional response surface plots were generated to illustrate variations in responses relative to process variables. Optimization was performed under the following constraints: maximizing expansion ratio and crispiness, while minimizing bulk density (BD) and hardness of the extrudates as shown in **Figure**.

3.2 Physical Properties of Extrudates

3.2.1 Expansion Ratio

The expansion ratio (ER) is an important quality indicator for extrudates and ready-to-eat puffed snacks, which can affect the texture, lightness, and overall consumer acceptance (Boakye et al., 2022; Chou & Hsu, 2021; Uribe-Wandurraga et al., 2020). Generally, feed moisture content, barrel temperature and screw speed are factors affecting the ER of the extrudates (Ali et al., 2024; Singha & Muthukumarappan, 2018). During extrusion, the pressurized melt exits the die into an environment with much lower atmospheric pressure, causing rapid flash-off of internal moisture. This process generates air pockets within the product, producing the characteristic porous and expanded structure (Altaf et al., 2021; Okunola et al., 2023). Products with higher ER and porosity are generally preferred because it is directly related to the product's degree of starch gelatinization and crispness, as they indicate efficient expansion, uniform air cell distribution, and desirable textural qualities such as crispness and lightness (Lyu et al., 2023; Mohammed et al., 2024; Sharma & Gujral, 2013). Ultimately, the extent of expansion depends on the vapor pressure difference between water in the melt and the surrounding atmosphere, as well as the structural integrity of the extrudate during puffing (Rani et al., 2021; R. K. R. Singh et al., 2014).

The regression equation obtained for ER represented in equation 7.

$$\text{Expansion ratio}=1.81 + 0.19X_1 - 0.22X_2 - 0.08X_3 - 0.13X_4 - 0.08X_1X_2 - 0.03X_1X_3 - 0.12X_1X_4 + 0.06X_2X_3 + 0.15X_2X_4 + 0.02X_3X_4 - 0.28X_1^2 - 0.06X_2^2 - 0.12X_3^2 - 0.22X_4 \ldots\ldots\ldots\ldots\ldots (7)$$

The ER model showed a positive effect of starch (X_1) but negative effects of moisture (X_2), screw speed (X_3), and temperature (X_4), with X_2X_4 being the only notable positive interaction. Significant quadratic terms indicated curvature, where ER decreased at extreme levels of all variables, suggesting the need for moderate extrusion conditions.

The ER values of the extrudates varied between 1.08 and 2.16 (**Table 4)**. Pea starch 30%, moisture 21%, screw speed 250 rpm and temperature 120°C resulted in the minimum expansion ratio whereas the maximum expansion ratio was achieved at pea starch 50%, feed moisture 19%, screw speed 250 rpm and extrusion temperature of 135◦C.

Similar expansion ratio trends have been reported for a variety of extruded products, including rice chickpea flour blends and rice cowpea composite snacks (Altaf et al., 2021; Okunola et al., 2023), potato starch based expanded snacks (Calvo-Lopez & Martinez-Bustos, 2017), intermediate wheatgrass products (Boakye et al., 2022), extruded barley ready-to-eat snacks (Chou & Hsu, 2021), corn starch passion fruit pulp snacks (Cortés et al., 2014), cereal-based snacks (Hashemian et al., 2025), lotus rhizome broken rice flour blends (Hussain et al., 2017), and blends of finger millet, sweet potato, and soybean composite flour (Mohammed et al., 2024).

In **Figure 2,** the 3D surface plots demonstrate the interactive effects of process variables on the expansion ratio. ER increased with higher starch content and moderate moisture but declined at excessive moisture levels. Screw speed showed a positive effect at lower temperatures, while higher temperatures combined with high screw speed slightly reduced ER. These interactions highlight the need to balance feed composition and processing conditions for optimal product expansion.

Van Hoan et al., (2010) reported that starch serves as the primary component forming the expanded matrix in extruded blends, the observed increase in starch content corresponded with a higher expansion ratio. Feed moisture, barrel temperature, and screw speed interactively influence the expansion ratio (ER) of extrudates. An increase in feed moisture enhanced ER, but further increase in moisture reduced expansion ratio, likely due to decreased melt elasticity and increased plasticity at higher moisture levels (B. Singh et al., 2015; Srivastava et al., 2012). Barrel temperature generally promoted expansion by increasing steam formation, though excessive heating lowered melt viscosity and risked structural collapse (Calvo-Lopez & Martinez-Bustos, 2017; Gopirajah & Muthukumarappan, 2018). Screw speed effects were temperature dependent, with ER increasing at 135 °C but decreasing at 150 °C, reflecting the balance between shear induced expansion and starch network degradation (Hussain et al., 2017; Rani et al., 2021). Similar interactions among moisture, temperature, and screw speed have been reported for various extruded products (Lyu et al., 2023; Oke et al., 2013).

The ANOVA for the expansion ratio model indicated a significant overall model fit ($p < 0.05$) with an F-value of 6.33 (**Table 5**). The lack-of-fit test was not significant ($p = 0.06$), confirming that the model adequately represented the experimental data. The residual error was minimal, suggesting good precision in the predicted responses.

The fitted model for ER (**Table 6**) exhibited significant linear effects for all four independent variables, with X_1 showing a positive influence ($p < 0.05$) and X_2, X_3, and X_4 exerting negative effects ($p < 0.05$ for X_2 and X_4; $p < 0.1$ for X_3. Among the quadratic terms, X_1^2, X_3^2, and X_4^2 were significant, indicating curvature in the response, particularly for X_1 and X_4 where ER peaked at intermediate levels and declined at the extremes. The interaction between X_2 and X_4 was the only significant interaction term ($p < 0.1$), suggesting that higher values of both factors slightly increased ER. The model demonstrated a good fit, with $R^2 = 0.88$ and adjusted $R^2 = 0.74$, and an adequate precision of 8.11, exceeding the threshold value of 4. However, the predicted R^2 was comparatively low (0.32), indicating reduced predictive ability for data points outside the experimental range.

3.2.2 Bulk Density

Bulk density (BD) is an important quality characteristic of expanded ready-to-eat products and an indicator of expansion, reflecting volumetric puffing in all directions and showing an inverse relationship with the expansion ratio (Delgado-Nieblas et al., 2019; Hussain et al., 2017; Rani et al., 2021). Products with lower BD are lighter, contain more air cells, and are generally more acceptable to consumers, whereas higher BD produces compact, less digestible snacks (Boakye et al., 2022; Mohammed et al., 2024). Beyond consumer perception, BD is also critical for quality control and packaging design, as it influences material requirements, product texture, and mouthfeel (Ali et al., 2024; Okunola et al., 2023).

Equation 8 represented the regression equation obtained for BD.

$$\text{Bulk density} = 0.14 - 0.00X_1 + 0.05X_2 - 0.02X_3 - 0.03X_4 - 0.03X_1X_4 - 0.03X_2X_3 - 0.02X_2X_4 + 0.00X_3X_4 + 0.03X_1^2 + 0.03X_2^2 + 0.04X_3^2 + 0.05X_4^2 \ldots\ldots (8)$$

The BD model indicated a strong positive effect of moisture (X_2) and negative effects of screw speed (X_3) and temperature (X_4), with significant quadratic terms (X_1^2, X_2^2, X_3^2, X_4^2) showing curvature in the response. Overall, BD increased with higher moisture but decreased under higher screw speed and temperature, with extreme values of variables leading to denser products.

The BD values of the extrudates ranged between 0.13 and 0.34 g/cm^3 (**Table 4**). Pea starch 50%, moisture 21%, screw speed 250 rpm and temperature 135°C yielded extrudates with the lowest bulk density of 0.13 g/cm^3 while extrusion parameters pea starch 50%, feed moisture 23%, screw speed 250 rpm and extrusion temperature of 120◦C produced extrudates of the highest bulk density of 0.34g/cm^3.

Rangira et al., (2020) reported bulk density values ranged from 0.12 to 0.35 g/cm^3 in low moisture extrusion of pea starch. Sahu et al., (2022) recorded bulk density values varied from 0.13 - 0.28 g/cm^3 the production of soy protein enriched maize based extruded snack. BD values observed in this study are consistent with previous reports on various extruded products, including lotus rhizome and broken rice flour blends (Hussain et al., 2017), potato starch-based expanded snacks (Calvo-Lopez & Martinez-Bustos, 2017), intermediate wheatgrass extrudates (Boakye et al., 2022), and finger millet sweet potato and soybean composites (Mohammed et al., 2024). Similar findings have also been recorded in cereal-based snacks supplemented with food by-products (Hashemian et al., 2025), rice-cowpea composites (Okunola et al., 2023), kodo millet and chickpea blends (Geetha et al., 2014), rice-chickpea blends, and tigernut-based snacks (Kalahal et al., 2024).

The 3D surface plots in **Figure 3** show the interactive effects of process variables on bulk density (BD). BD decreased with increasing starch content and moderate screw speed but rose again at higher levels of these factors. Moisture and temperature also showed curvature effects, where higher values tended to increase BD, indicating reduced expansion. These interactions demonstrate that excessive moisture or high thermal mechanical input leads to denser, less expanded products, while balanced conditions resulted lower density extrudates.

Bulk density (BD) of extrudates is strongly influenced by feed moisture, screw speed, and barrel temperature. Higher feed moisture reduces melt elasticity through plasticization, lowering SME and expansion, and thus increasing BD (Altaf et al., 2021; Chanlat et al., 2011; Hashemian et al., 2025; Mohammed et al., 2024; B. Singh et al., 2015). In contrast, higher screw speeds lower melt viscosity, improve elasticity, and promote puffing, leading to reduced BD, although excessive shear may degrade starch and limit expansion (Boakye et al., 2022; Hussain et al., 2017; Ye et al., 2018). Barrel temperature also plays a key role, where increased heating enhances starch gelatinization, superheating of water, and flash-off at the die, resulting in larger alveoli, greater expansion, and lower BD (Ali et al., 2024; Geetha et al., 2014; Okunola et al., 2023). However, very high temperatures or high fiber/protein levels may destabilize bubble walls, cause cell collapse, or induce crosslinking, thereby increasing density (Kalahal et al., 2024; Lyu et al., 2023). Overall, BD shows a quadratic response to moisture and temperature, initially decreasing with improved expansion and gelatinization, but increasing at excessive levels due to reduced dough elasticity and structural collapse (Ding et al., 2006; Singha & Muthukumarappan, 2018).

In **Table 5** the ANOVA for the bulk density model indicated a significant overall fit ($p < 0.01$; $F = 7.25$), confirming that the selected variables adequately explained the variation in BD. The lack-of-fit test was not significant ($p = 0.14$), suggesting good agreement between predicted and experimental values. The low residual error further supports the reliability and precision of the model.

The fitted model for bulk density (BD) **Table 6** showed a significant positive linear effect of moisture (X_2) and negative linear effects of screw speed (X_3) and temperature (X_4). Interaction effects were limited, with X_1X_4 and X_2X_3 significantly reducing BD. The quadratic terms for X_2^2, X_3^2, and X_4^2 were positive and significant, indicating curvature in the response, with BD decreasing at moderate levels but increasing again at higher values. The model explained the variability well ($R^2 = 0.89$; adjusted $R^2 = 0.77$), and the predicted R^2 (0.40) indicated moderate predictive accuracy. Adequate precision (9.25) exceeded the threshold value of 4, confirming a strong signal-to-noise ratio and reliability of the model.

3.2.3 Hardness

Hardness, defined as the maximum force required to fracture an extrudate, is a key quality attribute influencing consumer acceptance (Ali et al., 2024; Charunuch et al., 2014). It is strongly linked with expansion and bulk density, where greater puffing lowers density and hardness, producing lighter and crispier textures (Blandino et al., 2022; Boakye et al., 2022; Calvo-Lopez & Martinez-Bustos, 2017). Lower hardness and breaking strength values are generally preferred, as excessive hardness diminishes crispness and consumer appeal (Altaf et al., 2021; Kalahal et al., 2024).

The regression equation obtained for the hardness of extrudates represented in equation 9.

$$\text{Hardness} = 41.58 - 6.64X_1 + 19.68X_2 - 11.45X_3 - 14.50X_4 - 14.07X_1X_2 + 11.77X_1X_3 - 14.27X_1X_4 - 1.11X_2X_3 - 6.45X_2X_4 + 11.21X_3X_4 + 10.22X_1^2 + 4.66X_2^2 + 3.11X_3^2 + 11.07X_4^2 \quad \ldots\ldots\ldots \quad (9)$$

The model indicates that hardness increased significantly with feed moisture (X_2), while screw speed (X_3) and temperature (X_4) exerted strong negative effects, reducing hardness. Several interaction terms (X_1X_2, X_1X_4, X_2X_4) also showed negative contributions, suggesting that combined increases in these variables lowered hardness further. Conversely, positive quadratic effects for all four factors indicated curvature in the response, where hardness tended to increase again at extreme levels of starch, moisture, screw speed, and temperature. This suggests that moderate operating conditions favored reduced hardness, while excessive values in either direction increased resistance to fracture.

The hardness of extrudates varied between 30.33 and 109.74 (N) as represented in **Table 4** Pea starch 70%, moisture 21%, screw speed 250 rpm and temperature 150°C produced extrudates with less hardness while extrusion parameters pea starch 30%, feed moisture 23%, screw speed 250 rpm and extrusion temperature of 135◦C yielded extrudates of more hardness.

In this study, the hardness of extrudates was consistent with reported values (40.07 to 99.96 N) in extrudates from rice-chickpea blends (Altaf et al., 2021). Comparable ranges have also been observed (20.39 to 57.12 N) for expanded intermediate wheatgrass products (Boakye et al., 2022), 23.8-53.3 N in pre-germinated extruded brown rice (Chanlat et al., 2011), and 70.44 to 122.1 N in extruded snacks from finger millet, sweet potato and soybean composites (Mohammed et al., 2024). Similar ranges were noted in rice starch amaranth expanded snacks (Castellanos-Gallo et al., 2019). While higher hardness values (421.1 to 503.0 N) have been documented in whole wheat extrudates (Bhat et al., 2019).

The 3D surface plots in **Figure 4** illustrate the interactive effects of process variables on hardness of extrudates. Hardness decreased with increasing screw speed and barrel temperature due to reduced melt viscosity and greater bubble growth, while higher feed moisture increased hardness by promoting denser structures. Interaction effects showed that combinations of high moisture with low screw speed, or low temperature with high screw speed, produced expanded products. Moderate processing conditions produced softer, more expanded products, whereas extreme values led to compact, harder extrudates.

Hardness of extrudates is influenced by screw speed, feed moisture, barrel temperature, starch, and fiber content (Castellanos-Gallo et al., 2019; Kalahal et al., 2024; Mohammed et al., 2024). High feed moisture acted as a plasticizer, reducing dough elasticity and increasing density and hardness (Boakye et al., 2022; Castellanos-Gallo et al., 2019), whereas low moisture promoted dextrinization and fragile cell walls, lowering hardness (Altaf et al., 2021). Increased screw speed and barrel temperature generally reduced hardness by lowering melt viscosity and enhancing bubble growth (Mohammed et al., 2024; Sahu et al., 2022), although excessive shear could toughen textures (Chou & Hsu, 2021). Hardness correlated positively with bulk density and negatively with expansion (Boakye et al., 2022; Chou & Hsu, 2021), while higher fiber levels further increased hardness by limiting starch gelatinization and bubble expansion (Bhat et al., 2019; Bordoloi & Ganguly, 2014).

The ANOVA for hardness in **Table 5** confirmed that the model was significant ($p < 0.01$; $F = 5.24$), indicating that the selected variables adequately explained the variation in response. The lack-of-fit was not significant ($p = 0.056$), suggesting good agreement between predicted and experimental values. The relatively low residual error further supports the reliability of the model.

The fitted model for hardness in **Table 6** showed a strong positive effect of feed moisture (X_2), while screw speed (X_3) and barrel temperature (X_4) had significant negative effects, reducing hardness. Significant interaction terms (X_1X_2, X_1X_4) also contributed negatively, indicating that combinations of starch with moisture or temperature reduced hardness further. Positive quadratic effects for all variables highlighted curvature in the response, where hardness tended to rise again at extreme processing conditions. The model explained 86% of the variability ($R^2 = 0.86$; adjusted $R^2 = 0.70$) with an adequate precision of 7.91, though the relatively low predicted R^2 (0.20) suggests limited predictive strength beyond the experimental range.

3.2.4 Crispiness

Crispness, a key texture attribute of RTE snacks, is perceived through a combination of tactile, kinesthetic, visual and auditory sensations generated by fracture of brittle cellular structures during eating (Ding et al., 2006; Mazumder et al., 2007). It is instrumentally measured by the number of positive peaks in force deformation curves and parameters such as crispness work, puncturing force, and rupture force, which correlate with sensory perception (Chanlat et al., 2011; Uribe-Wandurraga et al., 2020). Moisture plays an important role, as even small increases in water content reduce crispness and consumer acceptability (Alam et al., 2016; Sahu et al., 2022). Studies confirm that crispness is closely related to extrudate cell structure, with puncture tests and rupture distance effectively quantifying brittleness (Ding et al., 2006).

Equation 10 denotes the regression equation obtained for crispiness of the extrudates.

$$\text{Crispiness} = 590.93 - 6.90X_1 + 62.78X_2 - 57.29X_3 - 95.42X_4 - 60.96X_1X_2 + 38.70X_1X_3 - 91.68X_1X_4 - 3.26X_2X_3 - 8.19X_2X_4 + 62.36X_3X_4 - 95.36X_1^2 - 47.59X_2^2 - 55.00X_3^2 - 74.49X_4^2 \quad \ldots\ldots (10)$$

The crispiness model showed a strong positive effect of moisture (X_2), while screw speed (X_3) and barrel temperature (X_4) had negative effects, reducing crispiness. Significant interaction and quadratic terms revealed curvature, indicating that extreme levels of variables decreased crispiness, whereas moderate processing conditions favored a lighter, more brittle texture.

The crispiness of the extrudates ranged between 284.68 and 751.43 N.s (**Table 4**). Pea starch 50%, moisture 21%, screw speed 200rpm and temperature 120°C produced extrudates with the highest crispiness while extrusion parameters pea starch 70%, feed moisture 21%, screw speed 250 rpm and extrusion temperature of 150◦C gave extrudates of lowest crispiness.

The 3D surface plots in **Figure 5** showed that crispiness increased with moderate feed moisture but decreased at higher screw speeds and barrel temperatures, reflecting the role of melt viscosity and bubble growth. Interaction effects indicated that combinations of high screw speed with lower moisture or temperature favored greater brittleness, while extreme conditions reduced crispiness by collapsing cell structures. Overall, moderate processing conditions promoted lighter, crispier textures, whereas excessive mechanical and thermal inputs produced denser, less brittle products.

Crispness of extrudates was strongly affected by extrusion variables, particularly feed moisture, barrel temperature, and screw speed. High feed moisture reduced crispness by plasticizing the dough, lowering elasticity, and producing compact structures (Ding et al., 2006; Mazumder et al., 2007; Sahu et al., 2022), whereas higher barrel temperature enhanced expansion and porosity, resulting in thinner cell walls and more brittle textures (Mohammed et al., 2024). Screw speed also improved crispness at elevated temperatures by promoting puffing and bubble formation (Geetha et al., 2014). Excessive dietary fiber and protein limited expansion by restricting starch gelatinization and water mobility, thereby reducing crispness (Beck et al., 2018; Castellanos-Gallo et al., 2019; Félix-Medina et al., 2020).

The ANOVA (**Table 5**) for crispiness showed that the model was significant ($p < 0.05$; $F = 3.49$), confirming that the process variables had a meaningful effect on crispness. The lack-of-fit was not significant ($p = 0.11$), indicating good agreement between predicted and experimental values. The relatively low residual error further supports the adequacy and reliability of the model.

The fitted model for crispiness (**Table 6**) indicated a positive effect of feed moisture (X_2), while screw speed (X_3) and barrel temperature (X_4) exerted significant negative effects, reducing crispiness. Interaction terms such as X_1X_4 and quadratic terms for all variables (X_1^2, X_2^2, X_3^2, X_4^2) were negative and significant, highlighting curvature and showing that extreme processing conditions lowered crispiness. The model explained 80% of the variability ($R^2 = 0.80$), though the adjusted R^2 (0.57) and negative predicted R^2 (−0.12) indicated limited predictive ability beyond the experimental range. Adequate precision (7.36) exceeded the threshold of 4, confirming that the model had an acceptable signal-to-noise ratio.

3.3 Optical Property of the Extrudates

3.3.1 Color

Color is an important quality attribute of extruded snacks, directly influencing consumer acceptance and serving as an indicator of the extent of thermal processing (Altaf et al., 2021; Jacques-Fajardo et al., 2017). It is commonly measured using the CIELAB scale (L*, a*, b*), with L* being particularly useful for assessing browning kinetics (Kalahal et al., 2024; Sharma & Gujral, 2013). Color changes during extrusion are mainly attributed to non-enzymatic browning reactions such as Maillard reactions and caramelization, along with pigment oxidation and degradation (Boakye, Okyere, Bharathi, et al., 2023; Pismag et al., 2024; Sukumar & Athmaselvi, 2019). Starch degradation into sugars and their interaction with free amino acids enhances these reactions, while protein and fiber may partially mitigate reductions in lightness (Singha et al., 2018; Zhang et al., 2020). Monitoring color parameters post-extrusion is thus essential to evaluate browning, pigment degradation, and overall product quality (Hashemian et al., 2025).

Equation 11 represents the regression equation obtained for the color of extrudates.

$$\text{Color} = 74.05 + 2.34X_1 + 0.41X_2 + 0.18X_3 + 0.47X_4 - 1.04X_1X_2 + 0.12X_1X_3 - 0.25X_1X_4 + 0.22X_2X_3 - 0.57X_2X_4 - 0.09X_3X_4 + 1.89X_1^2 + 0.87X_2^2 + 0.31X_3^2 + 1.40X_4^2 \ldots\ldots\ldots\ldots\ldots\ldots (11)$$

The color (L*) model showed positive linear effects of starch (X_1), moisture (X_2), screw speed (X_3), and temperature (X_4), while negative interaction terms (X_1X_2, X_2X_4) indicated some combined effects reducing lightness. Significant quadratic terms for all variables reflected curvature in the response, with color improving at moderate conditions but declining under extremes due to intensified browning reactions.

The L* values of the extrudates ranged between 72.71 and 80.55 (**Table 4**). In this study, the L* values of extrudates were comparable to ranges reported in previous studies. Ali et al., (2024) observed L* values between 74.08 and 79.79, while tigernut-based snacks showed values of 68.86 to 74.30 (Kalahal et al., 2024). Broader ranges of lightness have been reported, such as 64.69 to 91.25 in extrudates from distiller's dried grains, garbanzo flour, and corn grits (Singha et al., 2018), 68.85 to 89.78 in rice–chickpea blends (Altaf et al., 2021), and 68.58 to 86.95 in corn extrudates with red lentil bran (Kesre & Masatcioglu, 2022). Lower L* values (58.32 to 70.12) were documented in cereal-based snacks enriched with by-products, reflecting higher browning intensity (Hashemian et al., 2025).

Extrusion conditions affected the color and appearance of extrudates. Higher barrel temperatures promoted Maillard and caramelization reactions between sugars and proteins, leading to reduced L* values and darker products (Ali et al., 2024; Altaf et al., 2021; Okunola et al., 2023; Singha et al., 2018). Increased temperature and feed moisture enhanced starch degradation and sugar amino interactions, further contributing to browning and pigment oxidation (Hashemian et al., 2025; Pismag et al., 2024; Zhang et al., 2020). High protein content favored Maillard reactions, while compact air cells at elevated moisture increased light absorption, darkening the extrudates (Altaf et al., 2021). In contrast, higher screw speeds shortened residence time, limiting browning and sometimes increasing the color (Pismag et al., 2024). Pigment degradation, particularly carotenoids, also contributed to the reduction in luminosity at higher temperatures (Kesre & Masatcioglu, 2022).

The ANOVA for color in **Table 5** showed that the model was significant ($p < 0.01$; $F = 5.68$), indicating that extrusion variables had a meaningful effect on color attributes. The lack-of-fit test was not significant ($p = 0.42$), confirming good agreement between predicted and experimental values. The relatively low residual error further supports the adequacy and reliability of the model. The surface plots showed that moderate starch, moisture, screw speed, and temperature maintained higher L* values, while extreme conditions reduced lightness. Higher barrel temperature and feed moisture promoted Maillard and caramelization reactions, darkening the extrudates. In contrast, intermediate screw speeds limited browning, helping preserve product luminosity.

For color (L*), the fitted model in **Table 6** recorded positive linear effects of starch (X_1), moisture (X_2), screw speed (X_3), and temperature (X_4), indicating that moderate increases in these variables enhanced lightness. Negative interaction effects (X_1X_2, X_2X_4) suggested that combined increases in starch-moisture or moisture-temperature reduced L* values, consistent with browning during extrusion. Significant quadratic terms for all variables (X_1^2, X_2^2, X_3^2, X_4^2) highlighted curvature, where extreme conditions decreased luminosity due to intensified Maillard and pigment-degradation reactions. The model explained 87% of the variation ($R^2 = 0.87$; adjusted $R^2 = 0.72$), with adequate precision (8.17) confirming model reliability, though the predicted R^2 (0.29) indicated only moderate predictive strength.

3.4 Hydrational Properties of Extrudates

3.4.1 Water Absorption and Water Solubility Indices

The water absorption index (WAI) and water solubility index (WSI) are key indicators of starch transformation during extrusion, reflecting the degree of gelatinization and degradation. WAI measures the water absorbed and retained as gel after starch swelling, serving as an index of starch digestibility and cooking quality (Alajil et al., 2020; Altaf et al., 2021; Hussain et al., 2017). In contrast, WSI quantifies the soluble polysaccharides released from starch, indicating molecular breakdown and dextrinization (Alam et al., 2016; Ding et al., 2006). Higher extrusion temperatures generally increase WSI by enhancing starch degradation and sugar-amino interactions, while protein and fiber may modulate these effects (Hashemian et al., 2025; Zhang et al., 2020). Low WSI values are desirable for breakfast cereals, which must retain crispness in milk, whereas higher WSI may be beneficial in baby foods requiring rapid solubility (Charunuch et al., 2014; Kowalski et al., 2015). Together, WAI and WSI provide essential insights into the functional properties, texture, and digestibility of extruded snacks (Boakye et al., 2022; Pismag et al., 2024).

The regression equations obtained for water absorption and water solubility indices are represented in equations 12 and 13 respectively.

$$WAI = 5.06 + 0.59X_1 + 0.34X_2 - 0.21X_3 - 0.00X_4 - 0.22X_1X_2 - 0.09X_1X_3 - 0.07X_1X_4 + 0.04X_2X_3 + 0.14X_2X_4 - 0.00X_3X_4 + 0.50X_1^2 - 0.02X_2^2 + 0.10X_3^2 - 0.04X_4^2 \ldots\ldots\ldots\ldots\ldots (12)$$

$$WSI = 26.95 - 0.96X_1 - 2.39X_2 - 1.86X_3 - 0.41X_4 - 0.72X_1X_2 - 0.93X_1X_3 - 0.73X_1X_4 - 0.70X_2X_3 - 1.88X_2X_4 - 0.12X_3X_4 - 2.99X_1^2 + 1.79X_2^2 + 0.27X_3^2 + 2.54X_4^2 \ldots\ldots\ldots\ldots\ldots\ldots (13)$$

The WAI model showed that starch (X_1) and moisture (X_2) had positive effects, while screw speed (X_3) reduced water absorption, indicating that higher starch and moisture promoted gelatinization whereas shear limited swelling. Significant interaction (X_1X_2) and quadratic terms (X_1^2, X_3^2) highlighted curvature, with WAI increasing under moderate conditions but declining at extremes. On the other hand, the WSI model revealed negative effects of X_1 and X_2, while X_3 and X_4 increased solubility, reflecting greater starch degradation under high shear and heat. Interaction effects (X_1X_2, X_2X_4) and quadratic terms (X_1^2, X_2^2, X_4^2) further confirmed that WSI rose with intense processing but declined at excessive starch or moisture levels. Together, these models demonstrate that WAI is favored by starch gelatinization under moderate processing, whereas WSI is promoted by molecular breakdown under higher thermal and mechanical inputs.

The values for WAI and WSI of the extrudates ranged between 4.49 to 6.59 g/g and 21.45 to 35.91% respectively (**Table 4**). Extrusion conditions of pea starch 30%, moisture 19 %, screw speed 250 rpm and temperature 135°C resulted minimum WAI while of pea starch 70%, moisture 21 %, screw speed 200 rpm and temperature 135°C maximized the WAI of extrudates. In contrast, extrusion parameters: pea starch 30%, moisture 23%, screw speed 250 rpm and temperature 135°C yielded low WSI while high WSI was reported on extrusion conditions pea starch 50%, feed moisture 19%, screw speed 250 rpm and extrusion temperature of 150◦C.

The WAI and WSI values in this study aligned well with literature ranges for extruded snacks. Reported WAI values include 5.77 to 6.40 g/g for quinoa (Alajil et al., 2020), 2.68 to 7.05 g/g for lotus-rice blends (Hussain et al., 2017), 3.7 to 4.5 g/g for wheatgrass (Boakye et al., 2022), 3.75 to 4.71 g/g for millet-soy blends (Mohammed et al., 2024), and up to 8.17 g/g for rice-chickpea snacks (Altaf et al., 2021). Similar values were also reported for kodo-chickpea (Geetha et al., 2014), by-product fortified snacks (Hashemian et al., 2025), rice-cowpea (Okunola et al., 2023), and soy-maize extrudates (Sahu et al., 2022). WSI values varied from 2.8 to 20% for rice-cowpea (Okunola et al., 2023) 16.65 to 32.75% for by-product fortified snacks (Hashemian et al., 2025), 12.59 to 20.93% for quinoa (Alajil et al., 2020), 15.91to 30.98% for intermediate wheatgrass extrudates (Boakye, Okyere, Bharathi, et al., 2023), and 9.05 to 18.87% for rice-chickpea blends (Altaf et al., 2021). Overall, WAI reflected starch gelatinization, while WSI indicated starch degradation, both strongly influenced by extrusion conditions and formulation.

Response surface plots **Figure 6** for WAI and **Figure** for WSI, indicated that WAI increased with starch and moisture content but decreased with higher screw speed due to shear-induced breakdown. On the other hand, WSI decreased at higher starch and moisture but increased significantly at high screw speed and temperature, showing enhanced dextrinization and solubility. This indicates that moderate extrusion conditions favor WAI through starch swelling, while extreme conditions enhance WSI through molecular degradation and enhanced solubility but also risk excessive breakdown.

The Water Absorption Index (WAI) and Water Solubility Index (WSI) were influenced by extrusion conditions, feed moisture, screw speed, and barrel temperature. WAI generally increased with higher feed moisture due to reduced melt viscosity and enhanced starch gelatinization, though excessive temperature or dextrinization reduced WAI by degrading starch polymers (Hussain et al., 2017; Mohammed et al., 2024; Sahu et al., 2022). Screw speed had mixed effects, lower shear preserved intact polymer chains and hydrophilic groups, increasing WAI, whereas higher speeds induced degradation, lowering absorption capacity (Altan et al., 2009; Okunola et al., 2023). In contrast, WSI rose with screw speed and temperature due to starch breakdown into smaller, soluble molecules under high shear and thermal energy, consistent with increased SME and amylopectin depolymerization (Boakye et al., 2022; Ding et al., 2006; Singha et al., 2018). High moisture often decreased WSI, as water plasticized the melt, reduced shear, and limited starch degradation, whereas low moisture enhanced solubility via greater macromolecular damage (Ali et al., 2024; Neder-Suárez et al., 2020). Protein and fiber further modified these responses by restricting gelatinization and promoting water retention, which enhanced WAI but reduced solubility (Altaf et al., 2021; Kalahal et al., 2024; Liu et al., 2017).

The ANOVA results in **Table 5** indicated that the fitted models for both WAI and WSI were highly significant ($p < 0.001$), with F-values of 19.74 and 6.45, respectively, confirming the strong influence of extrusion variables. The lack-of-fit tests were not significant for either WAI ($p = 0.058$) or WSI ($p = 0.655$), suggesting that the models adequately described the data. These results validate the predictive capability of the quadratic models, showing that WAI was more strongly explained by process variables compared to WSI, as reflected by its higher model F-value.

The fitted model for WAI in **Table 6**, the showed a strong fit ($R^2 = 0.96$, Adj $R^2 = 0.91$, Pred $R^2 = 0.76$), with X_1 and X_2 exerting significant positive effects, while X_3 had a negative impact. Quadratic terms (X_1^2, X_3^2) further highlighted curvature, indicating that excessive starch or screw speed reduced WAI after reaching optimum levels. The high Adeq Precision (16.87) confirmed excellent signal-to-noise ratio, validating model reliability.

The fitted model for WSI (**Table 6**), the model was also significant ($R^2 = 0.88$, Adj $R^2 = 0.75$, Pred $R^2 = 0.40$), with X_2 reducing solubility, while X_3 and X_4 increased it, reflecting starch degradation under high shear and heat. Interaction effects (X_1X_2, X_2X_4) were also important, showing that combined variable changes influenced solubility. Although the Pred R^2 was moderate, Adeq Precision (10.15) indicated a sufficiently strong signal, making the model acceptable.

3.5 Processing Response

3.5.1 Specific Mechanical Energy

Specific Mechanical Energy (SME), defined as the energy transferred from the motor per unit mass of extruded material, is a key extrusion parameter influencing extrusion efficiency, starch gelatinization, structural transformation, and product expansion (Hussain et al., 2017; Lyu et al., 2023; Rangira et al., 2020). Higher SME enhances starch conversion and expansion by increasing shear and reducing melt viscosity, though excessive inputs may cause macromolecular breakdown and alter viscoelastic properties (Ding et al., 2006; Jebalia et al., 2019; Pietsch et al., 2019). As it reflects screw speed, feed rate, torque, and viscosity, SME is widely used to optimize extrusion conditions and predict product quality (Beck et al., 2018; Lyu et al., 2023; Philipp et al., 2017).

Equation 14 represented the regression equation obtained for the specific mechanical energy of the extrusion processing.

$$SME = 884.13+58.38X_1 - 103.10X_2 + 162.36X_3 - 66.13X_4 - 41.40X_1X_2 + 12.81X_1X_3 - 8.35X_1X_4 + 1.88X_2X_3 + 26.80X_2X_4 - 11.92X_3X_4 - 30.99X_1^2 + 13.14X_2^2 - 20.10X_3^2 - 20.57X_4^2 \text{.........} \quad (14)$$

The fitted model for SME showed significant effects of all four independent variables, with positive contributions from X_1 and X_3, while higher X_2 and X_4 reduced SME. Interaction terms such as X_1X_2 and X_2X_4 also influenced SME, while quadratic effects (X_1^2, X_3^2, X_4^2) indicated nonlinear responses. The predicted SME values ranged around 884.13 kJ/kg under optimized extrusion conditions.

The SME was reported in the range of 586.40 to1132.09 KJ/Kg (**Table 4**). Extrusion condition pea starch 30%, moisture 21%, screw speed 200rpm and temperature 135°C resulted lower SME while extrusion parameters pea starch 50%, feed moisture 19%, screw speed 300 rpm and extrusion temperature of 135◦C caused higher SME.

SME values reported in extrusion studies vary widely depending on material and conditions. For instance, ranges of 147.89 to 320.22 KJ/kg were observed in lotus rhizome rice blends (Hussain et al., 2017), 213.98 to 539.35 KJ/kg in blue corn, pea, and oat bran extrudates (Jacques-Fajardo et al., 2017), and 64.38 to 138.71 kJ/kg in extrudates from pea starch (Rangira et al., 2020). Higher SME values (100 to 2000 kJ/kg) and (503 to 1276 kJ/kg) were reported in pea protein and starch composites respectively (Chen et al., 2021; Jebalia et al., 2019, 2022), while Boakye et al. (2023) found 352.84 to 491.53 kJ/kg in intermediate wheatgrass extrudates. Similarly, Beck et al. (2018) reported SME of 558 kJ/kg for pea protein fiber and rice starch blends.

The response surface plots **Figure** illustrated how specific mechanical energy (SME) responds to changes in extrusion process variables. SME was significantly influenced by extrusion conditions, increasing with screw speed and barrel temperature while decreasing with feed moisture. Maximum SME values were observed at high screw speed and low moisture, reflecting enhanced shear and energy transfer. These conditions promoted greater starch degradation and expansion in the extrudates.

SME was influenced by extrusion variables, higher feed moisture and temperature generally reduce SME due to their plasticizing and lubricating effects, which lower dough viscosity and torque requirements (Hussain et al., 2017; Rangira et al., 2020). Conversely, increasing screw speed raises SME by generating higher shear stress and mechanical energy transfer (Boakye, Okyere, Bharathi, et al., 2023; Lyu et al., 2023; Zahari et al., 2023). Elevated SME is often associated with greater starch gelatinization, structural transformation, and improved expansion of extrudates (Okunola et al., 2023; Philipp et al., 2017). However, excessive SME may induce molecular degradation, lowering melt viscosity (Jebalia et al., 2019). Interactions among process variables indicate that high SME values typically occur at low moisture, low barrel temperature, and high screw speed, conditions that maximize shear stress within the barrel (Heredia-Olea et al., 2020; Kesre & Masatcioglu, 2022).

The ANOVA results in **Table 5** for SME showed that the quadratic model was highly significant ($p < 0.0001$), with an F-value of 44.4, indicating that extrusion variables strongly influenced SME. The lack of fit was not significant ($p = 0.119$), confirming that the model adequately represented the data. This suggests that the developed regression model reliably explained the variation in SME across different processing conditions.

The fitted model for SME in **Table 6** showed that feed moisture (X_2) and extrusion temperature (X_4) had significant negative effects, meaning higher levels of these factors reduced SME. In contrast, screw speed (X_3) had the strongest positive effect, confirming that higher screw speeds increase SME due to greater shear input. Pea starch (X_1) also contributed positively, though to a lesser extent. Among quadratic terms, X_1^2 and X_4^2 showed negative influences, suggesting diminishing effects at extreme levels. For Specific Mechanical Energy (SME), the regression model ($R^2 = 0.98$, Adjusted $R^2 = 0.96$, Predicted $R^2 = 0.89$, Adeq Precision = 23.74) showed an excellent fit, indicating strong predictive reliability.

3.6 Optimization

The optimum conditions for each individual response and their predicted values along with desirability are given in **Table 7**, while the overall optimization of the extrusion processing for RTE snacks with optimized responses (high expansion, low bilk density, lower hardness, and more crispiness) are presented in **Table 8**. Design-Expert R © software was used for multi-response optimization. JMP software student version 18 was used for graphical presentation of the optimized data **Figure**. At the optimized extrusion conditions of 54.34% pea starch, 19.57% feed moisture, 240.79 rpm screw speed, and 131.42 °C barrel temperature, the model predicted desirable product characteristics with high overall desirability of 0.73. The expansion ratio (2.05) and low bulk density (0.13 g/cm³) indicated good puffing, while the WAI (5.07 g/g) and WSI (28.43%) reflected favorable hydration and starch conversion properties. The extrudates were expected to exhibit hardness (36.91 N) and high crispiness (556.30 N·sec), suggesting brittle texture suitable for snack products. A relatively high SME (970.69 kJ/kg) was associated with enhanced starch transformation under these conditions. The lightness of color ($L^* = 74.84$). The overall optimization achieved a balance of structural, textural, and functional attributes appropriate for ready-to-eat extrudates.

4. Conclusion

This research experiment aimed to optimize extrusion conditions for the development of expanded intermediate wheatgrass (IWG) snacks by varying pea starch level, feed moisture, screw speed, and barrel temperature with application of response surface methodology (RSM). The results showed that all variables influenced the physical, texture, and hydration properties of the extrudates. Expansion ratio improved with higher starch and screw speed, whereas increased feed moisture promoted compact structures and higher bulk density. Hydration indices (WAI and WSI) reflected starch gelatinization and degradation, with screw speed and temperature enhancing solubility. Hardness and crispness were strongly linked to expansion and density, while SME served as a key indicator of starch conversion and product quality. Color changes, mainly reductions in L* values, were attributed to Maillard browning and pigment degradation at higher temperature and moisture. The optimum conditions (54.34% pea starch, 19.57% feed moisture, 240.79 rpm screw speed, and 131.42 °C barrel temperature) produced extrudates with desirable functional and sensory properties. The study establishes the potential of IWG as a sustainable raw material for expanded ready-to-eat snacks and cereals, providing insights for both small- and large-scale food industries to design nutrient-rich products with improved consumer acceptability. The results provide a framework for commercializing Kernza®-based products, supporting both nutritional innovation and sustainability in cereal processing.

ACKNOWLEDGMENT

The authors would like to acknowledge PURIS (811 Glenwood Ave, Suite 110, Minneapolis, MN 55405, USA) for providing pea starch which is an important material used in this research.

AUTHOR CONTRIBUTIONS

Hazrat Usman: Conceptualization; Data curation; Formal analysis; Investigation; Writing-original draft and editing. **Cecia Flores-Sanchez**: Assisted in extrusion processing and analysis. **George A. Annor**: Idea; Conceptualization; Funding acquisition; Supervision; Writing-review and editing.

CONFLICTS OF INTEREST

The authors declare no conflict of interest.

FUNDING: This research was funded by Forever Green Initiative, University of Minnesota

DATA AVAILABILITY STATEMENT

The data generated and analyzed during the current study are available from the corresponding author upon reasonable request.

5. Tables

Table 1 Independent variables and their corresponding coded and actual levels for IWG-pea starch extrusion

Independent variables	Symbols	Coded levels		
		-1	0	+1
		Actual levels		
Pea Starch (%)	X_1	19	21	23
Moisture (%)	X_2	30	50	70
Screw Speed (rpm)	X_3	200	250	300
Temperature (℃)	X_4	120	135	150

-1= lowest level of independent variables, 0= midst level of independent variables and +1= highest level of independent variables
Abbreviations: IWG= intermediate wheatgrass and rpm=revolutions per minute

Table 2 Temperature setting in the six heating zones of the extruder

Barrel end temperature [℃]	Zone 1[℃]	Zone 2[℃]	Zone 3[℃]	Zone 4[℃]	Zone 5[℃]	Zone 6[℃]
120	50	80	120	120	120	120
135	50	80	120	135	135	153
150	50	80	120	150	150	150

Table 3 Variable combinations as determined using a Box-Behnken design coupled with response surface methodology (RSM)

Run	Variables code				Actual variables			
	X_1	X_2	X_3	X_4	Pea starch (%)	Feed moisture (%)	Screw speed (rpm)	Temperature (°C)
1	-1	+1	0	0	30	23	250	135
2	0	-1	0	-1	50	19	250	120
3	+1	+1	0	0	70	23	250	135
4	0	0	-1	-1	50	21	200	120
5	-1	0	0	+1	30	21	250	150
6	0	0	+1	+1	50	21	300	150
7	+1	0	0	+1	70	21	250	150
8	0	-1	+1	0	50	19	300	135
9	0	+1	0	-1	50	23	250	120
10	+1	0	0	-1	70	21	250	120
11	-1	0	+1	0	30	21	300	135
12	0	0	+1	-1	50	21	300	120
13	0	0	-1	+1	50	21	200	150
14	0	-1	0	+1	50	19	250	150
15	0	+1	-1	0	50	23	200	135
16	0	+1	0	+1	50	23	250	150
17	+1	0	-1	0	70	21	200	135

18	0	0	0	0	50	21	250	135
19	0	0	0	0	50	21	250	135
20	+1	-1	0	0	70	19	250	135
21	-1	-1	0	0	30	19	250	135
22	0	-1	-1	0	50	19	200	135
23	-1	0	0	-1	30	21	250	120
24	-1	0	-1	0	30	21	200	135
25	+1	0	+1	0	70	21	300	135
26	0	0	0	0	50	21	250	135
27	0	+1	+1	0	50	23	300	135

X_1=Pea starch, X_2=Feed moisture, X_3=Screw speed and X_4=Extrusion temperature. -1= lowest level of independent variables, 0= midst level of independent variables and +1= highest level of independent variables

Abbreviations: rpm=revolutions per minute

Table 4 Experimental values of the response variables from independent variables combinations using Box-Behnken design coupled with response surface methodology (RSM)

Run	X_1	X_2	X_3	X_4	ER	BD (g/cm3)	WAI (g/g)	WSI (%)	Hardness (N)	Crispiness (N.s)	SME (KJ/Kg)	Color (L*)
1	-1	+1	0	0	1.12^{a}	0.25^{cdefg}	5.75^{hijk}	21.45$^{a\ B}$	109.74$^{e\ A}$	639.19^{fgh}	764.40^{cdef}	76.00^{bcdefghi}
2	0	-1	0	-1	2.16$^{i\ A}$	0.16^{abc}	4.81^{abc}	32.34^{ijk}	39.25^{ab}	464.76^{abcdefg}	1070.91^{ij}	74.86^{abcdef}
3	+1	+1	0	0	1.29^{ab}	0.22^{abcdef}	6.30 ^{kl}	23.10^{abcde}	56.04^{abc}	394.53^{abcdef}	793.18^{defg}	79.68^{kl}
4	0	0	-1	-1	1.63^{cdefghi}	0.29^{efg}	5.64^{ghij}	25.99^{abcdef}	104.70^{de}	751.43$^{h\ A}$	749.62^{cde}	74.50^{abcd}
5	-1	0	0	+1	1.25^{ab}	0.21^{abcde}	5.01^{abcde}	29.08^{fghij}	53.53^{abc}	379.42^{abcd}	748.06^{bcde}	74.82^{abcdef}
6	0	0	+1	+1	1.17^{a}	0.17^{abcd}	4.74^{abc}	32.92^{jk}	34.22^{ab}	293.92^{a}	946.94^{hi}	77.69^{fghijkl}
7	+1	0	0	+1	1.42^{abcdef}	0.18^{abcde}	6.09^{jkl}	25.76^{abcdef}	30.33$^{a\ B}$	284.68$^{a\ B}$	815.83^{defgh}	78.45^{hijkl}
8	0	-1	+1	0	1.91^{ghi}	0.16^{abcd}	4.65^{ab}	32.13^{hijk}	30.92^{a}	480.18^{abcdefg}	1132.09$^{j\ A}$	73.33^{ab}
9	0	+1	0	-1	1.44^{abcdef}	0.34$^{g\ A}$	5.14^{bcdef}	31.00^{ghij}	100.87^{de}	664.66^{gh}	828.72^{defgh}	76.48^{cdefghij}
10	+1	0	0	-1	1.73^{cdefghi}	0.28^{efg}	6.08^{jkl}	22.75^{abc}	88.73^{cde}	626.23^{efgh}	924.34^{gh}	79.20^{jkl}
11	-1	0	+1	0	1.10^{a}	0.20^{abcde}	4.87^{abcd}	28.00^{fghi}	40.83^{ab}	325.99^{ab}	901.40^{fgh}	74.61^{abcde}
12	0	0	+1	-1	1.35^{abcd}	0.26^{defg}	4.95^{abcde}	31.57^{ghijk}	50.48^{ab}	413.99^{abcdef}	1105.47^{j}	76.38^{cdefghij}
13	0	0	-1	+1	1.39^{abcde}	0.19^{abcde}	5.44^{efghi}	26.87^{bcdefg}	43.59^{ab}	381.93^{abcde}	638.76^{abc}	76.15b^{bcdefghi}
14	0	-1	0	+1	1.37^{abcde}	0.19^{abcde}	4.57^{ab}	35.91$^{k\ A}$	33.67^{ab}	311.61^{a}	847.03^{defgh}	77.59^{efghijkl}
15	0	+1	-1	0	1.36^{abcde}	0.33^{fg}	5.47^{fghi}	27.57^{defgh}	57.98^{abc}	483.14^{abcdefg}	609.06^{ab}	75.55^{abcdefgh}
16	0	+1	0	+1	1.23^{ab}	0.28^{efg}	5.44^{efghi}	27.05^{cdefg}	69.48^{bcd}	478.75^{abcdefg}	712.04^{abcd}	76.95^{defghij}
17	+1	0	-1	0	1.8^{efghi}	0.25^{cdefg}	6.59$^{l\ A}$	22.90^{abcd}	52.46^{abc}	499.93^{abcdefg}	715.01^{abcd}	77.95^{ghijkl}
18	0	0	0	0	1.86^{fghi}	0.13$^{a\ B}$	5.01^{abcde}	24.99^{abcdef}	38.09^{ab}	625.03^{defgh}	885.02^{efgh}	75.01^{abcdefg}
19	0	0	0	0	1.80^{efghi}	0.15^{abc}	5.07^{abcdef}	28.85^{fghij}	45.086^{ab}	579.06^{cdefgh}	895.28^{fgh}	73.24^{ab}
20	+1	-1	0	0	1.80^{efghi}	0.14^{ab}	5.90^{ijk}	27.77^{efghi}	36.28^{ab}	376.44^{abc}	1084.46^{ij}	80.55$^{l\ A}$
21	-1	-1	0	0	1.32^{abc}	0.17^{abcd}	4.49$^{a\ B}$	28.99^{fghij}	33.70^{ab}	377.25^{abc}	890.07^{fgh}	72.71$^{a\ B}$
22	0	-1	-1	0	1.98^{hi}	0.16^{abcd}	4.96^{abcde}	29.31^{fghij}	34.32^{ab}	423.46^{abcdefg}	834.32^{defgh}	75.22^{abcdefg}
23	-1	0	0	-1	1.08$^{a\ B}$	0.21^{abcde}	4.72^{ab}	29.00^{fghij}	54.84^{abc}	354.23^{abc}	823.17^{defgh}	74.58^{abcde}
24	-1	0	-1	0	1.34^{abcd}	0.25^{bcdefg}	5.05^{abcde}	22.24^{ab}	95.66^{de}	584.62^{cdefgh}	586.40$^{a\ B}$	74.00^{abcd}
25	+1	0	+1	0	1.46^{abcdef}	0.20^{abcde}	6.06^{jkl}	24.94^{abcdef}	44.73^{ab}	396.11^{abcdef}	1081.24^{ij}	79.03^{ijkl}
26	0	0	0	0	1.78^{defghi}	0.15^{abc}	5.10^{bcdef}	27.01^{cdefg}	41.56^{ab}	568.71^{bcdefgh}	872.08^{efgh}	73.89^{abc}

27	0	+1	+1	0	1.51^{abcdefg}	0.21^{abcde}	5.31^{cdefg}	27.60^{defgh}	50.15^{ab}	526.83^{abcdefgh}	914.33^{gh}	74.53^{abcd}

X_1=Pea starch, X_2=Feed moisture, X_3=Screw speed and X_4=Extrusion temperature. -1= lowest level of independent variables, 0= midst level of independent variables and +1= highest level of independent variables
Results for each response are the means of multiple determinations of the samples run independently in duplicates.
Abbreviations: ER=Expansion ration, BD= Bulk density in grams per cubic centimeter, WAI= Water Absorption Index, WSI= Water Solubility Index, N= Newtons, N.s =Newton-second, SME (kJ/kg) = Specific Mechanical Energy in kilojoules per kilogram and L* = Lightness
Note: The lowercase superscript alphabet represents the significant difference ($p < 0.05$) between the mean values of each response in the column.
The uppercase superscript alphabet A and B in each response column indicates the highest and lowest mean values response variables.

Table 5 Analysis of variance (ANOVA) for best-fit models for response

Source	Sum of squares	Degrees of freedom	Mean square	*F* value	*p* Value	Remarks
Expansion ratio						
Model	2.02	14.00	0.14	6.33	0.00	significant
Residual	0.27	12.00	0.02			
Lack of fit	0.27	10.00	0.03	15.60	0.06	not significant
Pure error	0.00	2.00	0.00			
Cor Total	2.30	26.00				
Bulk Density						
Model	0.0768	14	0.0055	7.25	0.0007	significant
Residual	0.0091	12	0.0008			
Lack of fit	0.0088	10	0.0009	6.61	0.1385	not significant
Pure error	0.0003	2	0.0001			
Total	0.0859	26				
WAI						
Model	8.14	14	0.5815	19.74	< 0.0001	significant
Residual	0.3535	12	0.0295			

Lack of fit	0.3493	10	0.0349	16.64	0.058	not significant
Pure error	0.0042	2	0.0021			
Cor Total	8.49	26				
WSI						
Model	292.85	14	20.92	6.45	0.0013	significant
Residual	38.91	12	3.24			
Lack of fit	31.45	10	3.15	0.8437	0.6548	not significant
Pure error	7.46	2	3.73			
Cor Total	331.76	26				
Hardness						
Model	13049.18	14	932.08	5.24	0.0033	significant
Residual	2134.11	12	177.84			
Lack of fit	2109.68	10	210.97	17.27	0.0559	not significant
Pure error	24.43	2	12.22			
Cor Total	15183.29	26				
Crispiness						
Model	3.27E+05	14	23381.7	3.49	0.0182	significant
Residual	80451.83	12	6704.32			
Lack of fit	78654.4	10	7865.44	8.75	0.1068	not significant
Pure error	1797.44	2	898.72			
Cor Total	4.08E+05	26				
SME						
Model	5.60E+05	14	39972.07	44.4	< 0.0001	significant
Residual	10802.57	12	900.21			
Lack of fit	10532.26	10	1053.23	7.79	0.119	not significant
Pure error	270.32	2	135.16			
Total	5.70E+05	26				
Color(L*)						
Model	101.64	14	7.26	5.68	0.0023	significant
Residual	15.34	12	1.28			

Lack of fit	13.74	10	1.37	1.71	0.4241	not significant
Pure error	1.6	2	0.8016			
Cor Total	117.32	26				

Abbreviations: ER=Expansion ration, BD= Bulk density in grams per cubic centimeter, WAI= Water Absorption Index, WSI= Water Solubility Index, SME (kJ/kg) = Specific Mechanical Energy in kilojoules per kilogram and L* = Lightness
Cor Total=Corrected Total

Table 6 Regression coefficient and coefficient of determination of for the model

Variables	**ER**	**BD (g/cm3)**	**WAI(g/g)**	**WSI (%)**	**Hardness(N)**	**Crispiness (N.s)**	**SME (KJ/Kg)**	**Color(L*)**
Intercept	1.81*	0.14*	5.06*	26.95*	41.58*	590.93*	884.13*	74.05*
X_1	0.19**	0.00	0.59**	-0.96*	-6.64	-6.90	58.38**	2.35**
X_2	-0.22**	0.05**	0.34**	-2.39**	19.68**	62.78**	-103.10**	0.41
X_3	-0.08*	-0.02**	-0.21**	1.86**	-11.45**	-57.29**	162.36**	0.18
X_4	-0.13**	-0.03	0.00	0.41	-14.50**	-95.42**	-66.13**	0.47
$X_1 X_2$	-0.08	0.00	-0.22**	0.72	-14.07*	-60.96	-41.40**	-1.04*
$X_1 X_3$	-0.03	0.00	-0.09	-0.93	11.78	38.70	12.81	0.12
$X_1 X_4$	-0.12	-0.03*	-0.07	0.73	-14.27*	-91.69**	-8.35	-0.25
$X_2 X_3$	0.06	-0.03**	0.04	-0.70	-1.11	-3.26	1.88	0.22
$X_2 X_4$	0.15*	-0.02	0.14	-1.88*	-6.45	-8.19	26.80*	-0.57
$X_3 X_4$	0.02	0.00	0.00	0.12	11.21	62.36	-11.92	-0.09
X_1^2	-0.28**	0.03**	0.50*	-2.99**	10.22	-95.36**	-30.99**	1.89**
X_2^2	-0.06	0.03**	-0.02	1.79**	4.66	-47.59	13.14	0.87*
X_3^2	-0.12*	0.04**	0.10	0.27	3.11	-55.00	-20.10	0.31
X_4^2	-0.22**	0.05**	-0.04	2.55**	11.07*	-74.49*	-20.57	1.40**
R^2	0.88	0.89	0.96	0.88	0.86	0.80	0.98	0.87
Adjusted R^2	0.74	0.77	0.91	0.75	0.70	0.57	0.96	0.72
Predicted R^2	0.32	0.40	0.76	0.40	0.20	-0.12	0.89	0.29
Adeq Precision	8.11	9.25	16.87	10.15	7.91	7.36	23.74	8.17

X1=Pea starch, X2=Feed moisture, X3=Screw speed and X4=Extrusion temperature. R2= Coefficient od determination, Adeq Precision= Adequate precision

Abbreviations: ER=Expansion ration, BD= Bulk density in grams per cubic centimeter, WAI= Water Absorption Index, WSI= Water Solubility Index, N= Newtons, N·s =Newton-second, SME (kJ/kg) = Specific Mechanical Energy in kilojoules per kilogram and L* = Lightness
Values without an asterisk are not significant $p \geq 0.1$
**Statistical significance at $p < 0.05$.
*Statistically significant at $0.05 \leq p < 0.1$

Table 7 Individual response optimization of the model

Response variables	**Optimum parameters**					
	Pea starch (%)	**Moisture (%)**	**Screw speed(rpm)**	**Temperature (°C)**	**Predicted values**	**Desirability**
ER	63.01	19.00	217.56	122.68	2.22 (2.53)	0.99
BD (g/cm3)	50.00	21.00	250.00	135.00	0.14 (0.18)	0.89
WAI(g/g)	50.00	21.00	250.00	135.00	5.06 (5.28)	1.00
WSI (%)	50.00	21.00	250.00	135.00	26.95 (29.22)	1.00
Hardness(N)	30.00	19.00	300.00	123.19	34.8 (43.38)	1.00
Crispiness (N.s)	49.81	22.57	200.00	120.00	705.47 (880.63)	0.86
SME (KJ/Kg)	50.00	21.00	250.00	135.00	884.13 (921.87)	1.00
Color(L*)	50.00	21.00	250.00	135.00	74.05 (5.47)	1.00

Abbreviations: ER=Expansion ration, BD= Bulk density in grams per cubic centimeter, WAI= Water Absorption Index, WSI= Water Solubility Index, N= Newtons, N·s =Newton-second, SME (kJ/kg) = Specific Mechanical Energy in kilojoules per kilogram and L* = Lightness
Note: Data in parenthesis indicated the upper predicated values.

Table 8 Optimum parameters and predicted values individual response at optimized conditions

Optimum parameters	Actual values	Desirability
Pea starch (%)	54.34	1.00
Moisture (%)	19.57	1.00
Screw speed(rpm)	240.79	1.00
Temperature (℃)	131.42	1.00
Response variables	**Predicted values**	**Overall Desirability**
ER	2.05	0.73
BD (g/cm3)	0.13	
WAI(g/g)	5.07	
WSI (%)	28.43	
Hardness(N)	36.91	
Crispiness (N.s)	556.30	
SME (KJ/Kg)	970.69	
Color(L*)	74.84	

Abbreviations: ER=Expansion ration, BD= Bulk density in grams per cubic centimeter, WAI= Water Absorption Index, WSI= Water Solubility Index, N= Newtons, N·sec =Newton-second, SME (kJ/kg) = Specific Mechanical Energy in kilojoules per kilogram and L* = Lightness

6. Figures

(a)

(b)

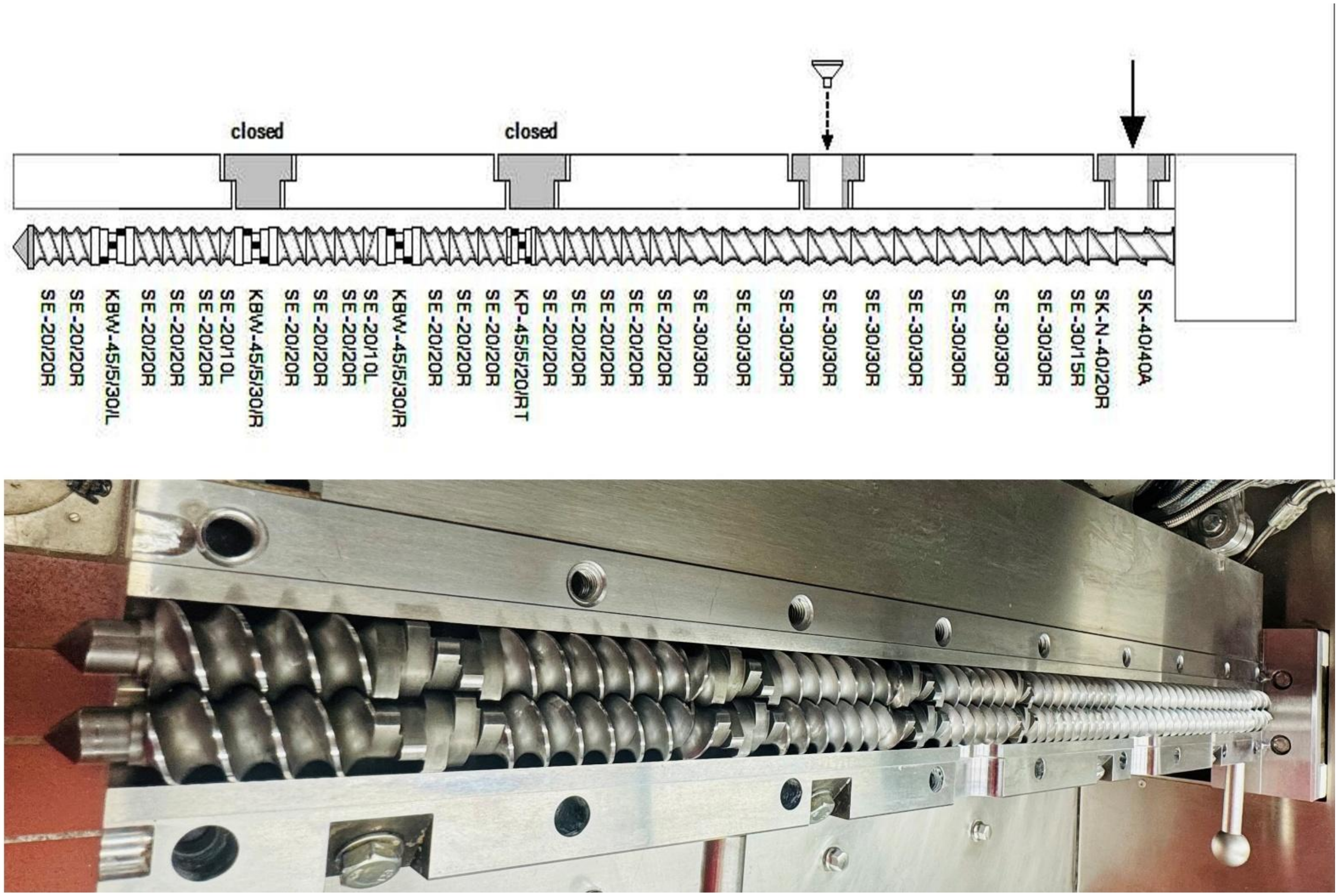

Figure 1: (a) Schematic representation of the screw configuration used in the extrusion processing. The configuration includes forward and reverse conveying screw elements, kneading blocks for mixing and shear development, and screw tips for final discharge.
Note: SE: normal screw profile, SK: thrust edge profile SK-N, thrust-edge-to-normal profile, first number: pitch in mm, second number: length in mm, R: conveying, L: Reverse conveying, A: feed element with undercut on the gear side, KB: kneading block, KBW: kneading block with a wide land. KP: kneading block with half disk width on both sides, first number: angular offset between the disks (°), second number: disks length in mm, third number: length in mm, T: twist, N: neutral kneading block.
(b) Picture of the Brabender® Twin-Screw used in extrusion processing, Department of Food Science and Nutrition, University of Minnesota.

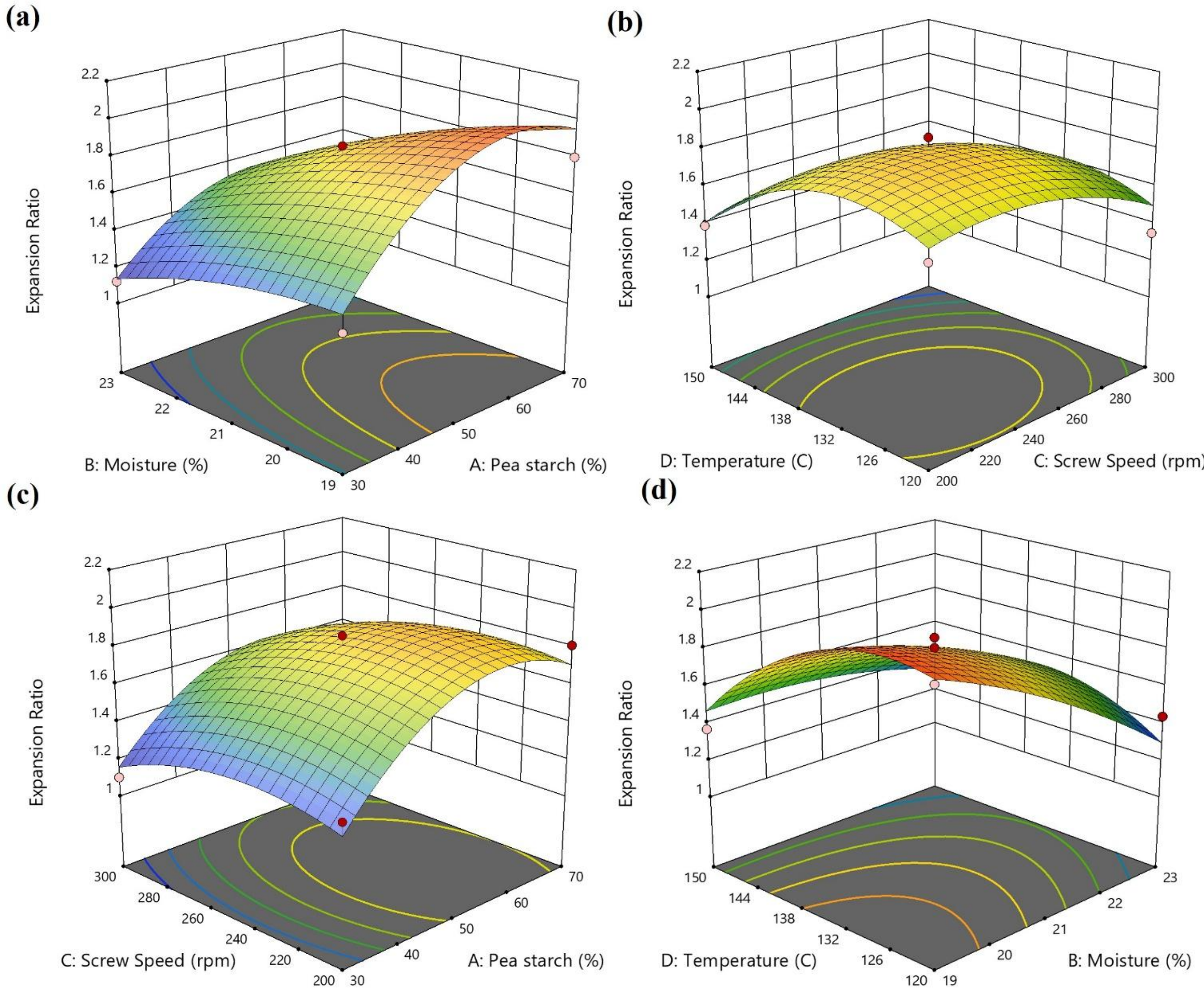

Figure 2: Three-dimensional surface plots for expansion ratio as impacted by different extrusion conditions at (a) temperature 135°C and screw speed 250 rpm, (b) pea starch 50% and moisture 21%, (c) moisture 21% and temperature 135°C (d) pea starch 50% and screw speed 250rpm.

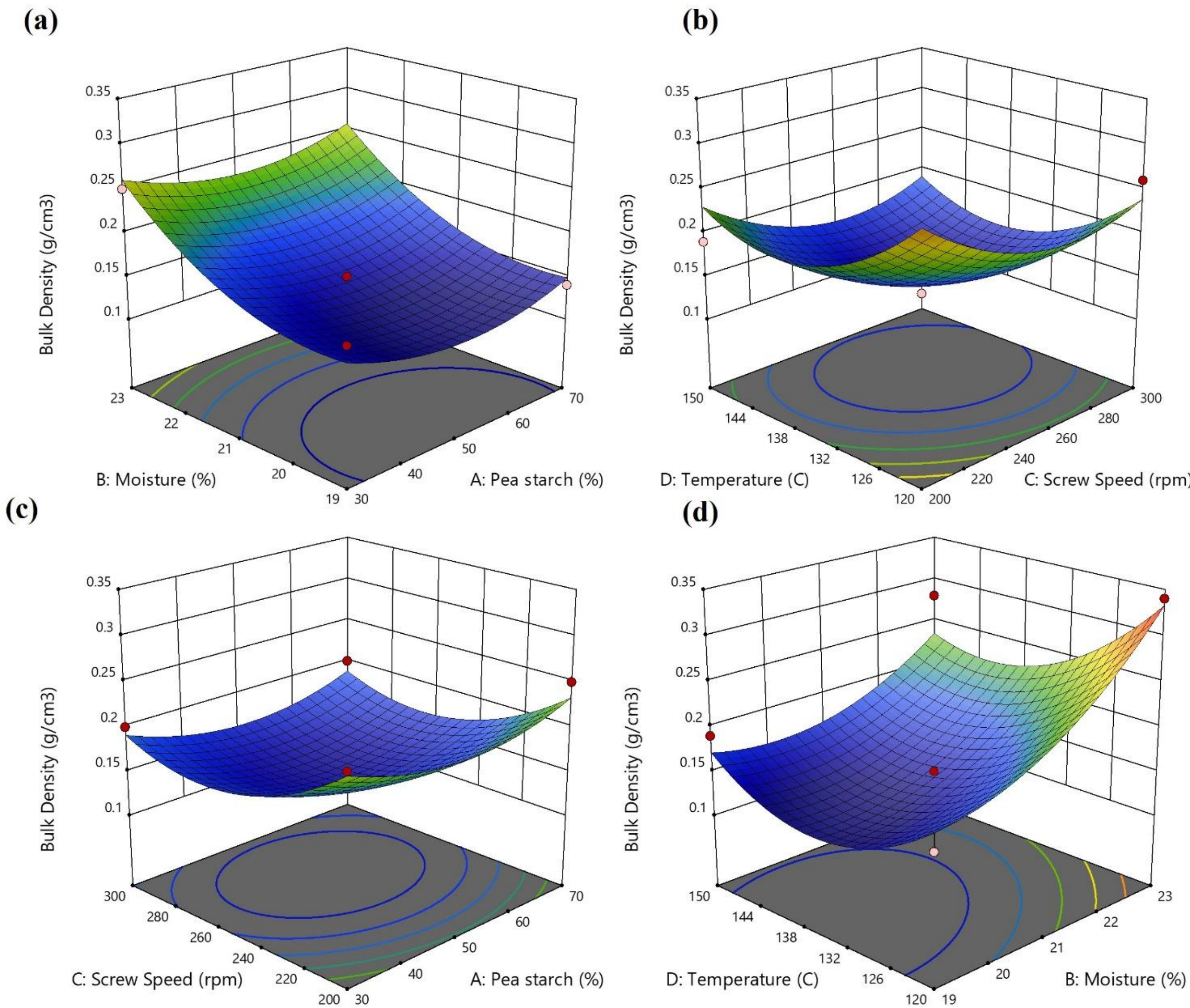

Figure 3: Three-dimensional surface plots for bulk density as impacted by different extrusion conditions at (a) at (a) temperature 135°C and screw speed 250 rpm, (b) pea starch 50% and moisture 21%, (c) moisture 21% and temperature 135°C (d) pea starch 50% and screw speed 250rpm.

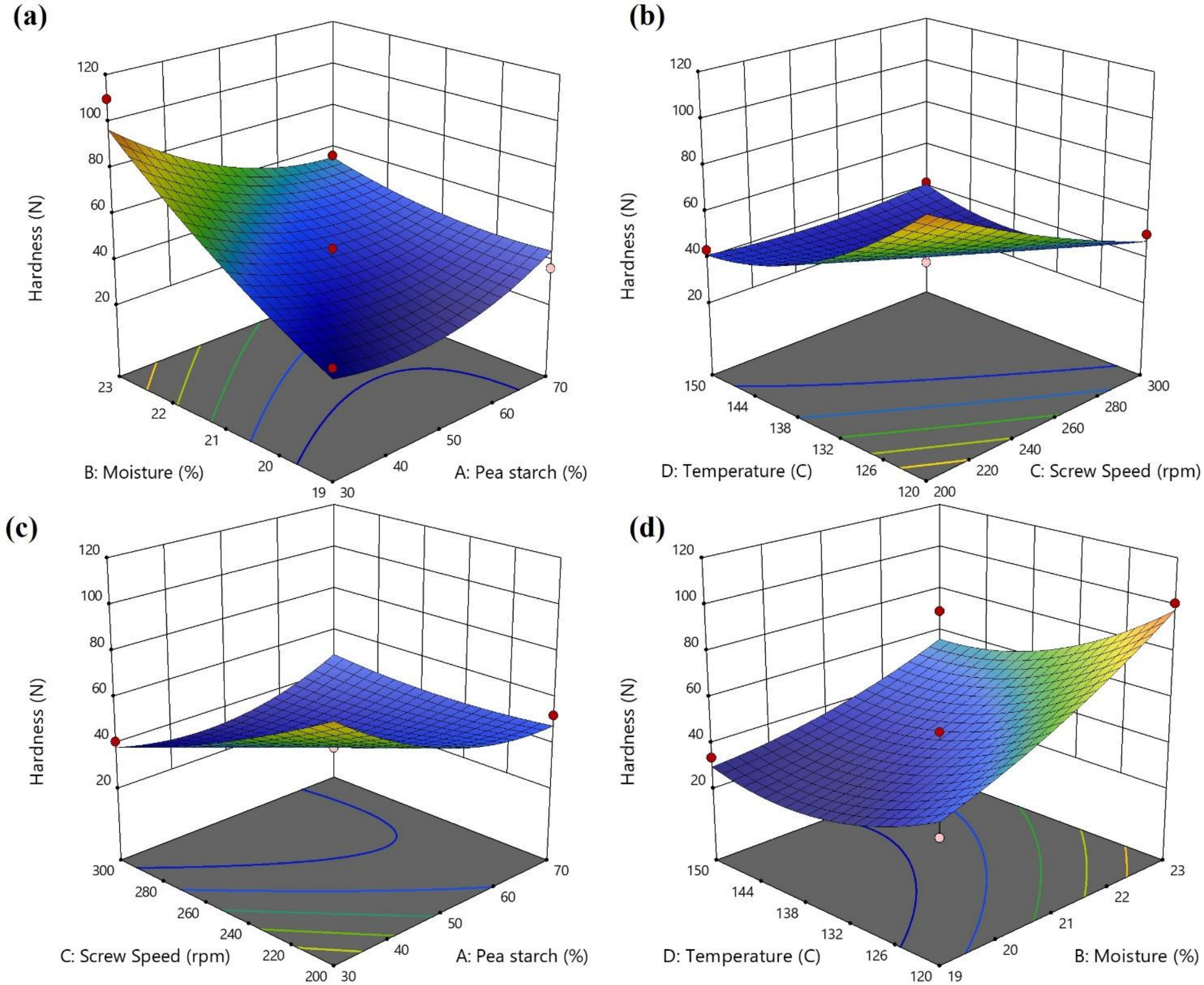

Figure 4: Three-dimensional surface plots for hardness as impacted by different extrusion conditions at (a) at (a) temperature 135°C and screw speed 250 rpm, (b) pea starch 50% and moisture 21%, (c) moisture 21% and temperature 135°C (d) pea starch 50% and screw speed 250rpm.

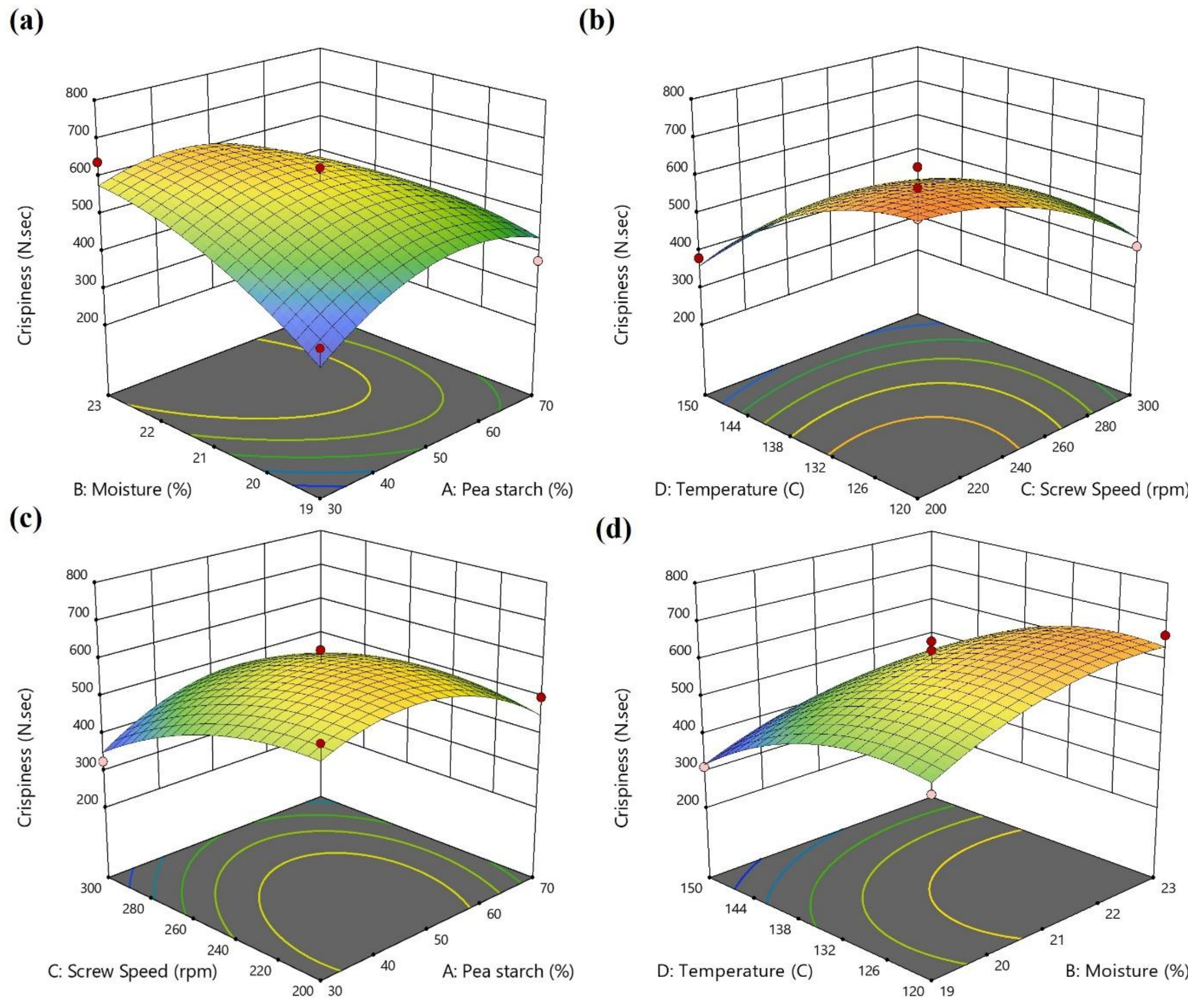

Figure 5: Three-dimensional surface plots for crispiness as impacted by different extrusion conditions at (a) at (a) temperature 135°C and screw speed 250 rpm, (b) pea starch 50% and moisture 21%, (c) moisture 21% and temperature 135°C (d) pea starch 50% and screw speed 250rpm.

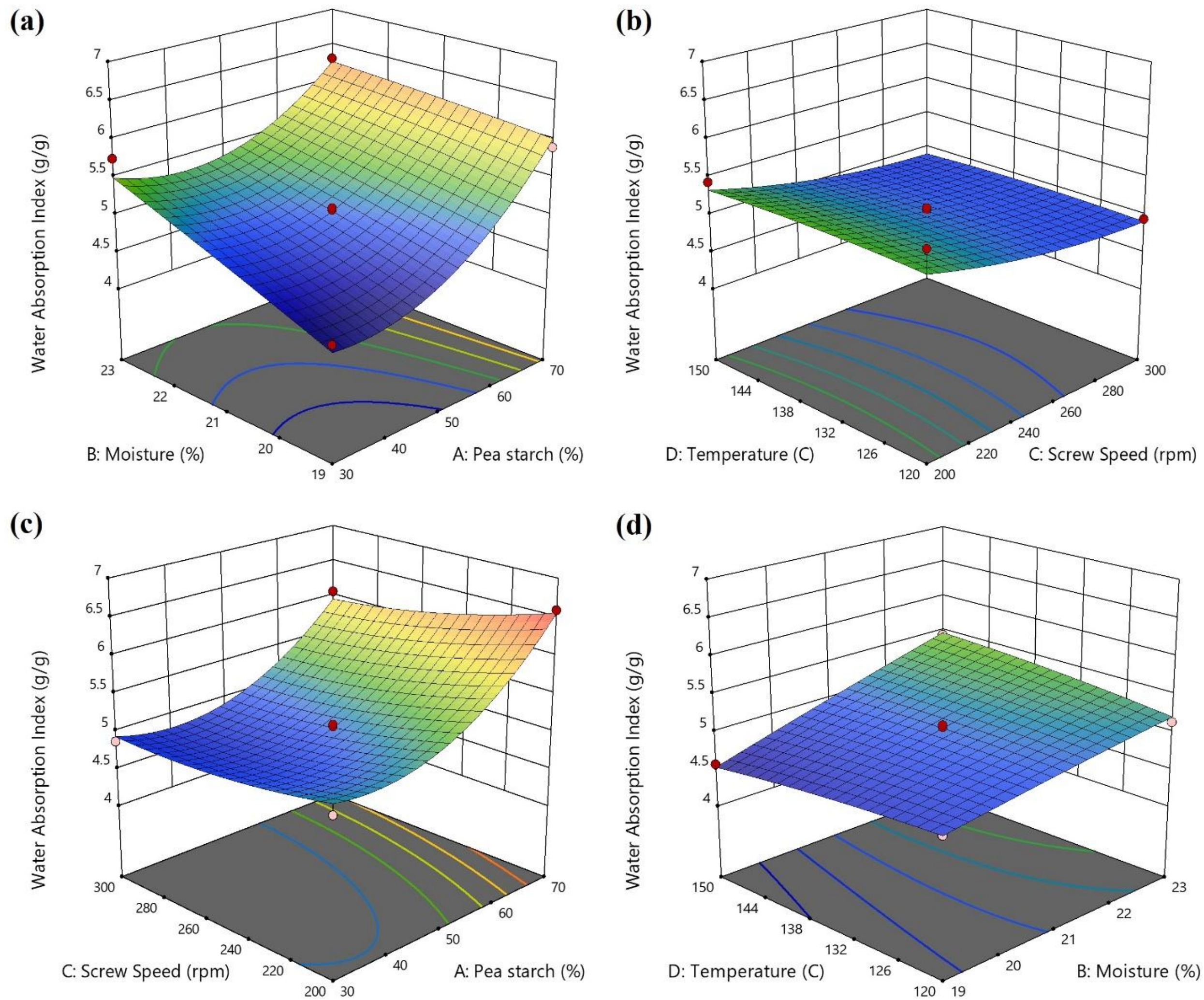

Figure 6: Three-dimensional surface plots for water absorption index as impacted by different extrusion conditions at (a) at (a) temperature 135°C and screw speed 250 rpm, (b) pea starch 50% and moisture 21%, (c) moisture 21% and temperature 135°C (d) pea starch 50% and screw speed 250rpm.

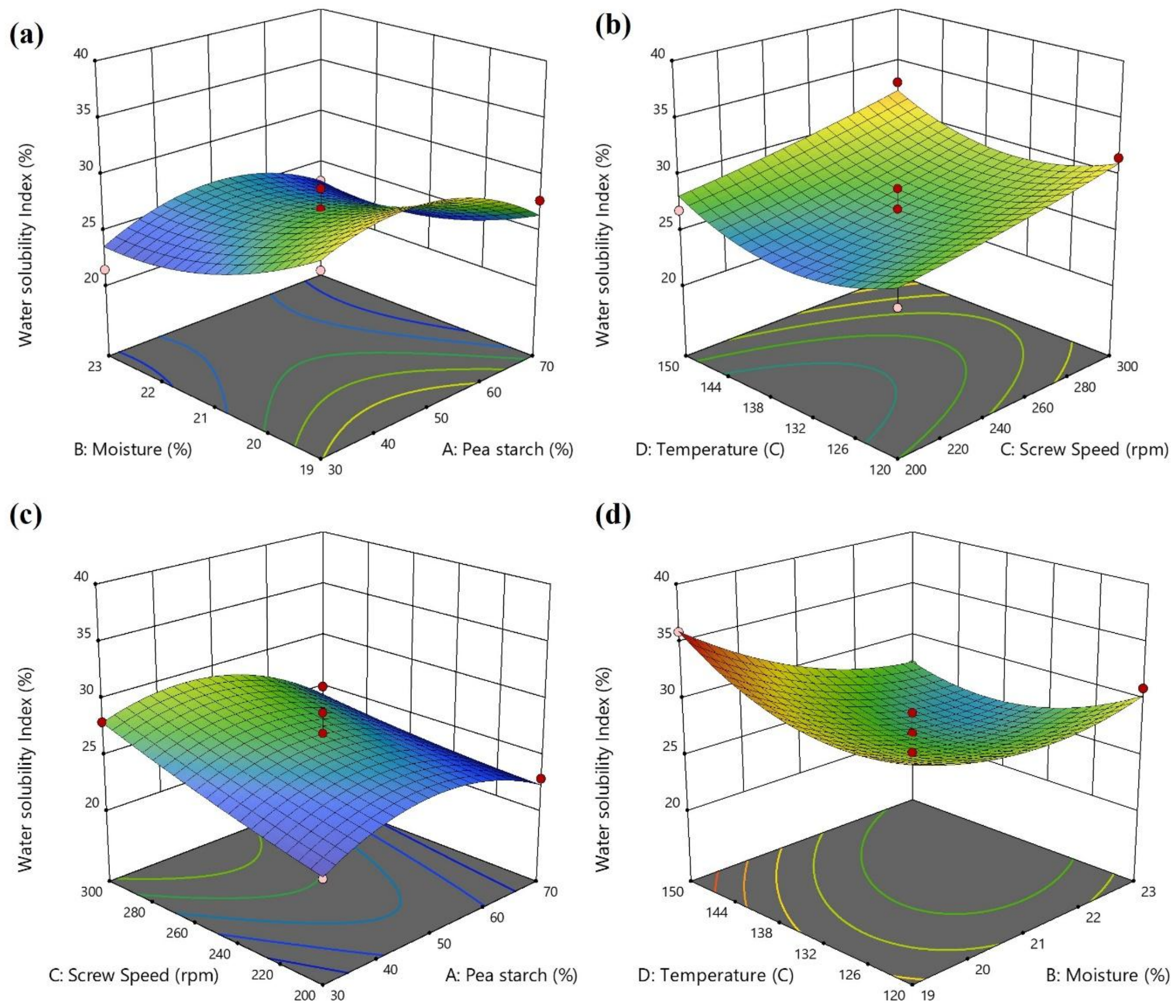

Figure 7: Three-dimensional surface plots for water solubility index as impacted by different extrusion conditions at (a) at (a) temperature 135°C and screw speed 250 rpm, (b) pea starch 50% and moisture 21%, (c) moisture 21% and temperature 135°C (d) pea starch 50% and screw speed 250rpm.

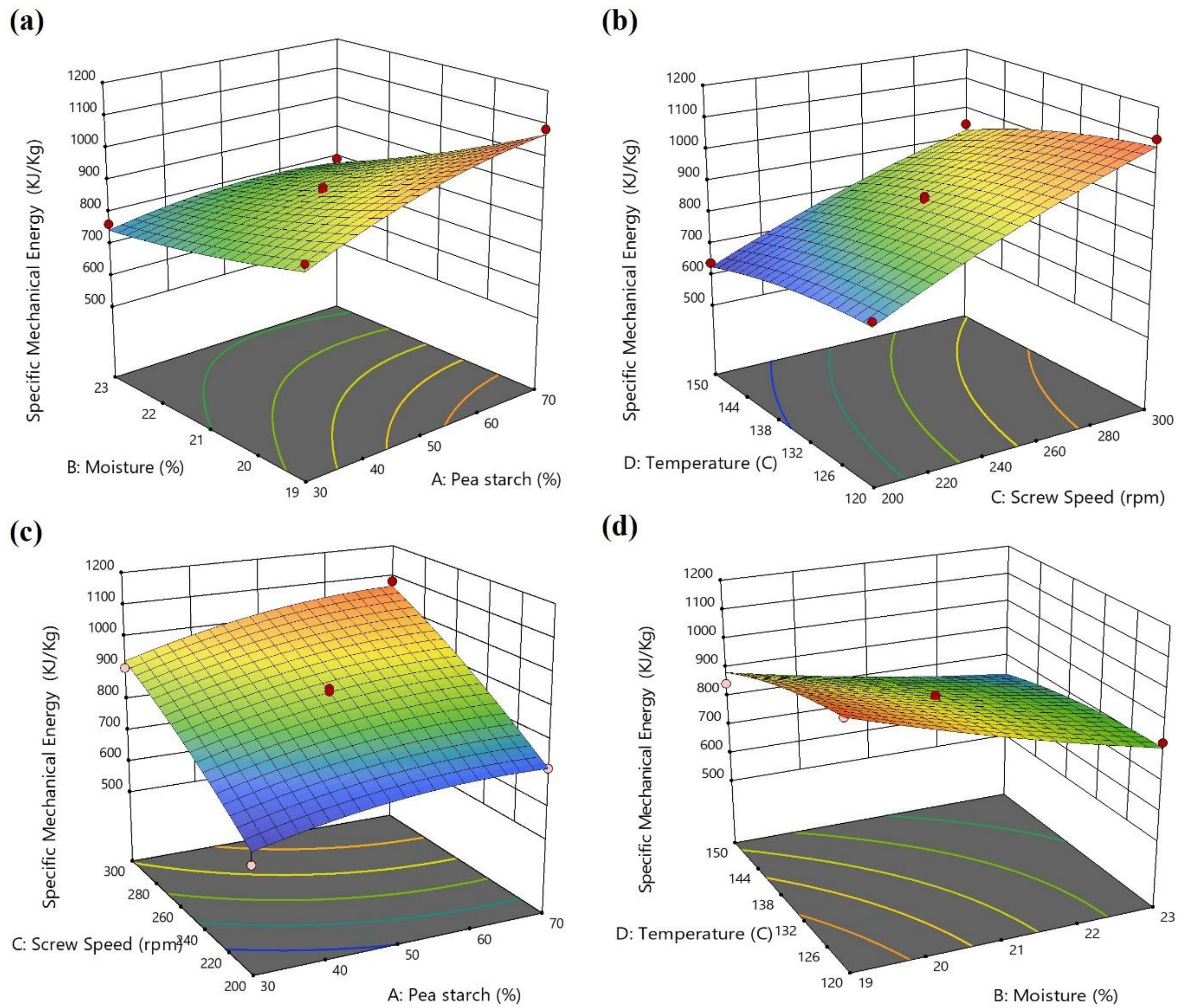

Figure 8: Three-dimensional surface plots for specific mechanical energy as impacted by different extrusion conditions at (a) at (a) temperature 135°C and screw speed 250 rpm, (b) pea starch 50% and moisture 21%, (c) moisture 21% and temperature 135°C (d) pea starch 50% and screw speed 250rpm.

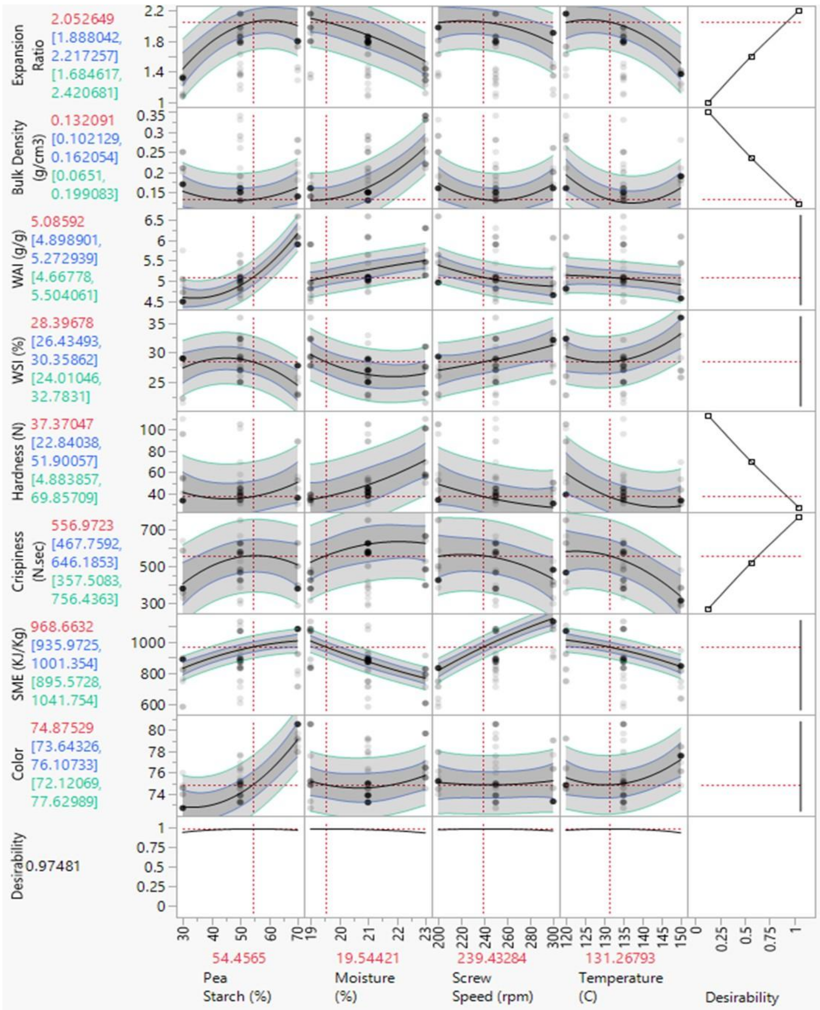

Figure 9: Predictions profiler of the optimized region for the extrusion processing parameters pea starch 54.33% and moisture 19.57%, (c) moisture 19.57%, screw speed 240.74rpm and temperature 131.41°C for producing extruded product and predicted values of the response variables overall desirability.

7. References

Alajil, O., Hymavathi, T. V., Maheswari, K. U., & Rudra, S. G. (2020). Nutritional, physico-chemical and sensory attributes of quinoa based extrudates. *Vegetos*, *33*(3), 390–400. https://doi.org/10.1007/s42535-020-00119-4

Alam, M. S., Kaur, J., Khaira, H., & Gupta, K. (2016). Extrusion and Extruded Products: Changes in Quality Attributes as Affected by Extrusion Process Parameters: A Review. *Critical Reviews in Food Science and Nutrition*, *56*(3), 445–473. https://doi.org/10.1080/10408398.2013.779568

Ali, I. M., Forsido, S. F., Kuyu, C. G., Ahmed, E. H., Andersa, K. N., Chane, K. T., & Regasa, T. K. (2024). Effects of extrusion process conditions on nutritional, anti-nutritional, physical, functional, and sensory properties of extruded snack: A review. *Food Science & Nutrition*, *12*(11), 8755–8761. https://doi.org/10.1002/fsn3.4472

Altaf, U., Hussain, S. Z., Qadri, T., Iftikhar, F., Naseer, B., & Rather, A. H. (2021). Investigation on mild extrusion cooking for development of snacks using rice and chickpea flour blends. *Journal of Food Science and Technology*, *58*(3), 1143–1155. https://doi.org/10.1007/s13197-020-04628-7

Annex 6—Glossary | Food Standards Agency. (n.d.). Retrieved July 20, 2025, from https://www.food.gov.uk/business-guidance/annex-6-glossary

Bajgain, P., Zhang, X., Jungers, J. M., DeHaan, L. R., Heim, B., Sheaffer, C. C., Wyse, D. L., & Anderson, J. A. (2020). 'MN-Clearwater', the first food-grade intermediate wheatgrass (Kernza perennial grain) cultivar. *Journal of Plant Registrations*, *14*(3), 288–297. https://doi.org/10.1002/plr2.20042

Beck, S. M., Knoerzer, K., & Arcot, J. (2017). Effect of low moisture extrusion on a pea protein isolate's expansion, solubility, molecular weight distribution and secondary structure as determined by Fourier Transform Infrared Spectroscopy (FTIR). *Journal of Food Engineering*, *214*, 166–174. https://doi.org/10.1016/j.jfoodeng.2017.06.037

Beck, S. M., Knoerzer, K., Foerster, M., Mayo, S., Philipp, C., & Arcot, J. (2018). Low moisture extrusion of pea protein and pea fibre fortified rice starch blends. *Journal of Food Engineering*, *231*, 61–71. https://doi.org/10.1016/j.jfoodeng.2018.03.004

Bhat, N. A., Wani, I. A., Hamdani, A. M., & Gani, A. (2019). Effect of extrusion on the physicochemical and antioxidant properties of value added snacks from whole wheat (*Triticum aestivum* L.) flour. *Food Chemistry*, *276*, 22–32. https://doi.org/10.1016/j.foodchem.2018.09.170

Blandino, M., Bresciani, A., Loscalzo, M., Vanara, F., & Marti, A. (2022). Extruded snacks from pigmented rice: Phenolic profile and physical properties. *Journal of Cereal Science*, *103*, 103347. https://doi.org/10.1016/j.jcs.2021.103347

Boakye, P. G., Okyere, A. Y., & Annor, G. A. (2023). Impact of extrusion processing on the nutritional and physicochemical properties of intermediate wheatgrass (*Thinopyrum intermedium*). *Cereal Chemistry*, *100*(3), 628–642. https://doi.org/10.1002/cche.10632

Boakye, P. G., Okyere, A. Y., Bharathi, R., Murai, T., & Annor, G. A. (2023). Physicochemical and nutritional properties of extruded products from cereals of the Triticeae tribe – A review. *Food Chemistry Advances*, *3*, 100379. https://doi.org/10.1016/j.focha.2023.100379

Boakye, P. G., Okyere, A. Y., Kougblenou, I., Kowalski, R., Ismail, B. P., & Annor, G. A. (2022). Optimizing the extrusion conditions for the production of expanded intermediate wheatgrass (*Thinopyrum intermedium*) products. *Journal of Food Science*, *87*(8), 3496–3512. https://doi.org/10.1111/1750-3841.16238

Bordoloi, R., & Ganguly, S. (2014). *EXTRUSION TECHNIQUE IN FOOD PROCESSING AND A REVIEW ON ITS VARIOUS TECHNOLOGICAL PARAMETERS*.

Brennan, M. A., Derbyshire, E., Tiwari, B. K., & Brennan, C. S. (2013). Ready-to-eat snack products: The role of extrusion technology in developing consumer acceptable and nutritious snacks. *International Journal of Food Science & Technology*, *48*(5), 893–902. https://doi.org/10.1111/ijfs.12055

Calvo-Lopez, A. D., & Martinez-Bustos, F. (2017). Optimization of Extrusion Process of Directly Expanded Snacks Based on Potato Starch in a Single Step for the Formation of Type IV Resistant Starch. *Plant Foods for Human Nutrition*, *72*(3).

Castellanos-Gallo, L., Galicia-García, T., Estrada-Moreno, I., Mendoza-Duarte, M., Márquez-Meléndez, R., Portillo-Arroyo, B., Soto-Figueroa, C., Leal-Ramos, Y., & Sanchez-Aldana, D. (2019). Development of an Expanded Snack of Rice Starch Enriched with Amaranth by Extrusion Process. *Molecules*, *24*(13), 2430. https://doi.org/10.3390/molecules24132430

Cetiner, B., Shamanin, V. P., Tekin-Cakmak, Z. H., Pototskaya, I. V., Koksel, F., Shepelev, S. S., Aydarov, A. N., Ozdemir, B., Morgounov, A. I., & Koksel, H. (2023). Utilization of intermediate wheatgrass (Thinopyrum intermedium) as an innovative ingredient in bread making. *Foods*, *12*(11), 2109.

Chadha, D., Young, O., Otter, D., & Kam, R. (2021). Physical analysis of friction cooked RTE snacks. *Innovative Food Science & Emerging Technologies*.

Chanlat, N., Songsermpong, S., Charunuch, C., & Naivikul, O. (2011). Twin-Screw Extrusion of Pre-Germinated Brown Rice: Physicochemical Properties and ?-Aminobutyric Acid Content (GABA) of Extruded Snacks. *International Journal of Food Engineering*, *7*(4). https://doi.org/10.2202/1556-3758.2328

Charunuch, C., Limsangouan, N., Prasert, W., & Wongkrajang, K. (2014). Optimization of extrusion conditions for ready-to-eat breakfast cereal enhanced with defatted rice bran. *International Food Research Journal*, *21*(2), 713.

Chen, Q., Zhang, J., Zhang, Y., Meng, S., & Wang, Q. (2021). Rheological properties of pea protein isolate-amylose/amylopectin mixtures and the application in the high-moisture extruded meat substitutes. *Food Hydrocolloids*, *117*, 106732. https://doi.org/10.1016/j.foodhyd.2021.106732

Choton, S., Gupta, N., Bandral, J. D., Anjum, N., & Choudary, A. (2020). Extrusion technology and its application in food processing: A review. *The Pharma Innovation Journal*, *9*(2), 162–168.

Chou, C. F., & Hsu, S. C. (2021). Effects of extrusion parameters on the physicochemical characteristics of extruded barley ready-to-eat snacks. *Journal of Food Processing and Preservation*, *45*(10), e15788. https://doi.org/10.1111/jfpp.15788

Clément, C., Sleiderink, J., Svane, S. F., Smith, A. G., Diamantopoulos, E., Desbrøll, D. B., & Thorup-Kristensen, K. (2022). Comparing the deep root growth and water uptake of intermediate wheatgrass (Kernza®) to alfalfa. *Plant and Soil*, *472*(1–2), 369–390. https://doi.org/10.1007/s11104-021-05248-6

Cortés, R. N. F., Guzmán, I. V., & Martínez-Bustos, F. (2014). Effects of Some Extrusion Variables on Physicochemical Characteristics of Extruded Corn Starch-passion Fruit Pulp (Passiflora edulis) Snacks. *Plant Foods for Human Nutrition*, *69*(4), 365–371. https://doi.org/10.1007/s11130-014-0443-8

Crain, J., Bajgain, P., Anderson, J., Zhang, X., DeHaan, L., & Poland, J. (2020). Enhancing Crop Domestication Through Genomic Selection, a Case Study of Intermediate Wheatgrass. *Frontiers in Plant Science*, *11*. https://doi.org/10.3389/fpls.2020.00319

Craine, E. B., & DeHaan, L. R. (2024). Nutritional Quality of Early-Generation Kernza Perennial Grain. *Agriculture*, *14*(6), 919. https://doi.org/10.3390/agriculture14060919

DeHaan, L., Christians, M., Crain, J., & Poland, J. (2018). Development and Evolution of an Intermediate Wheatgrass Domestication Program. *Sustainability*, *10*(5), Article 5. https://doi.org/10.3390/su10051499

Delgado-Nieblas, C., Ruiz-Beltrán, K., Sánchez-Lizárraga, J., Zazueta-Morales, J. D. J., Aguilar-Palazuelos, E., Carrillo-López, A., Camacho-Hernández, I. L., & Quintero-Ramos, A. (2019). Effect of extrusion on physicochemical, nutritional and antioxidant properties of breakfast cereals produced from bran and dehydrated naranjita pomace. *CyTA - Journal of Food*, *17*(1), 240–250. https://doi.org/10.1080/19476337.2019.1566276

Dey, D., Singh, G., Ishwarya, P., & Mateen, A. (2024). Functionality and Extrusion Processing of Millets—A Review. *Food Reviews International*, *40*(10), 3605–3633. https://doi.org/10.1080/87559129.2024.2367643

Ding, Q.-B., Ainsworth, P., Plunkett, A., Tucker, G., & Marson, H. (2006). The effect of extrusion conditions on the functional and physical properties of wheat-based expanded snacks. *Journal of Food Engineering*, *73*(2), 142–148. https://doi.org/10.1016/j.jfoodeng.2005.01.013

Favre, J. R., Castiblanco, T. M., Combs, D. K., Wattiaux, M. A., & Picasso, V. D. (2019). Forage nutritive value and predicted fiber digestibility of Kernza intermediate wheatgrass in monoculture and in mixture with red clover during the first production year. *Animal Feed Science and Technology*, *258*, 114298. https://doi.org/10.1016/j.anifeedsci.2019.114298

Félix-Medina, J. V., Montes-Ávila, J., Reyes-Moreno, C., Perales-Sánchez, J. X. K., Gómez-Favela, M. A., Aguilar-Palazuelos, E., & Gutiérrez-Dorado, R. (2020). Second-generation snacks with high nutritional and antioxidant value produced by an optimized extrusion process from corn/common bean flours mixtures. *LWT*, *124*, 109172. https://doi.org/10.1016/j.lwt.2020.109172

Food Extrusion Market: Trends, Growth, Analysis and Forecast (2021-2026). (2015). MarketsandMarkets. Retrieved July 20, 2025, from https://www.marketsandmarkets.com/Market-Reports/food-extrusion-market-221423108.html

Förster, A., Michl, K., Berg, G., Cernava, T., & Emmerling, C. (2025). Decomposition of Litter and Root Residues From Perennial Intermediate Wheatgrass Governed by the Soil Microbiome and Different Earthworm Species. *Journal of Sustainable Agriculture and Environment*, *4*(2). https://doi.org/10.1002/sae2.70068

Geetha, R., Mishra, H. N., & Srivastav, P. P. (2014). Twin screw extrusion of kodo millet-chickpea blend: Process parameter optimization, physico-chemical and functional properties. *Journal of Food Science and Technology*, *51*(11), 3144–3153. https://doi.org/10.1007/s13197-012-0850-5

Ginot, C., Bathellier, C., David, C., Rossing, W. A. H., Celette, F., & Duchene, O. (2024). Introducing intermediate wheatgrass as a perennial grain crop into farming systems: Insights into the decision-making process of pioneer farmers. *Agronomy for Sustainable Development*, *44*(6). https://doi.org/10.1007/s13593-024-00993-1

Glover, J. D., Reganold, J. P., Bell, L. W., Borevitz, J., Brummer, E. C., Buckler, E. S., Cox, C. M., Cox, T. S., Crews, T. E., Culman, S. W., DeHaan, L. R., Eriksson, D., Gill, B. S., Holland, J., Hu, F., Hulke, B. S., Ibrahim, A. M. H., Jackson, W., Jones, S. S., … Xu, Y. (2010). Increased Food and Ecosystem Security via Perennial Grains. *Science*, *328*(5986), 1638–1639. https://doi.org/10.1126/science.1188761

Gopirajah, R., & Muthukumarappan, K. (2018). Effect of extrusion process conditions on the physical properties of tef-oat healthy snack extrudates. *Journal of Food Processing and Preservation*, *42*(3), e13559. https://doi.org/10.1111/jfpp.13559

Grandal, S., Rieder, A., Dessev, T., Ballance, S., Tyl, C., & Koga, S. (2025). Flour composition, dough, and bread properties of intermediate wheatgrass (Thinopyrum intermedium) compared to annual wheat species. *Food Chemistry*, *474*, 143205. https://doi.org/10.1016/j.foodchem.2025.143205

Hashemian, S., Elhamirad, A. H., Milani, E., Shafafi Zenoozian, M., & Armin, M. (2025). Functional ready-to-eat cereal-based snacks supplemented with food by-products. *Journal of Food Science and Technology*. https://doi.org/10.1007/s13197-025-06247-6

Heredia-Olea, E., Contreras-Alvarado, M. D., Perez-Carrillo, E., Rosa-Millán, J. D. L., & Serna-Saldivar, S. O. (2020). Assessment of the techno-functionality, starch digestion rates and protein quality of rice flour–whey protein instant powders produced in a twin extruder. *International Journal of Food Science & Technology*, *55*(2), 878–890. https://doi.org/10.1111/ijfs.14376

Hussain, S. Z., Ali, F., Jabeen, R., & Zargar, I. (2017). *Twin Screw Extrusion Cooking of Lotus Rhizome and Broken Rice Flour Blends: A Response Surface Analysis*. *76*.

Jacques-Fajardo, G. E., Prado-Ramírez, R., Arriola-Guevara, E., Pérez Carrillo, E., Espinosa-Andrews, H., & Guatemala Morales, G. M. (2017). Physical and hydration properties of expanded extrudates from a blue corn, yellow pea and oat bran blend. *LWT*, *84*, 804–814. https://doi.org/10.1016/j.lwt.2017.06.046

Jebalia, I., Della Valle, G., & Kristiawan, M. (2022). Extrusion of pea snack foods and control of biopolymer changes aided by rheology and simulation. *Food and Bioproducts Processing*, *135*, 190–204. https://doi.org/10.1016/j.fbp.2022.08.001

Jebalia, I., Maigret, J.-E., Réguerre, A.-L., Novales, B., Guessasma, S., Lourdin, D., Della Valle, G., & Kristiawan, M. (2019). Morphology and mechanical behaviour of pea-based starch-protein composites obtained by extrusion. *Carbohydrate Polymers*, *223*, 115086.

Kalahal, S. P., Gavahian, M., & Lin, J. (2024). Development of innovative tigernut-based nutritional snack by extrusion process: Effects of die temperature, screw speed, and formulation on physicochemical characteristics. *Quality Assurance and Safety of Crops & Foods*, *16*(1), Article 1. https://doi.org/10.15586/qas.v16i1.1310

Kearney, J. (2010). Food consumption trends and drivers. *Philosophical Transactions of the Royal Society B: Biological Sciences*, *365*(1554), 2793–2807. https://doi.org/10.1098/rstb.2010.0149

Kesre, C., & Masatcioglu, M. T. (2022). Physical characteristics of corn extrudates supplemented with red lentil bran. *LWT*, *153*, 112530. https://doi.org/10.1016/j.lwt.2021.112530

Kowalski, R. J., Morris, C. F., & Ganjyal, G. M. (2015). Waxy Soft White Wheat: Extrusion Characteristics and Thermal and Rheological Properties. *Cereal Chemistry*, *92*(2), 145–153. https://doi.org/10.1094/CCHEM-03-14-0039-R

Kristiawan, M., Micard, V., Maladira, P., Alchamieh, C., Maigret, J.-E., Réguerre, A.-L., Emin, M. A., & Della Valle, G. (2018). Multi-scale structural changes of starch and proteins during pea flour extrusion. *Food Research International*, *108*, 203–215. https://doi.org/10.1016/j.foodres.2018.03.027

Law, E. P., Wayman, S., Pelzer, C. J., DiTommaso, A., & Ryan, M. R. (2022). Intercropping red clover with intermediate wheatgrass suppresses weeds without reducing grain yield. *Agronomy Journal*, *114*(1), 700–716. https://doi.org/10.1002/agj2.20914

Liu, L., Li, S., Zhong, Y., Li, Y., Qu, J., Feng, J., Xu, S., Zhang, R., Xue, J., & Guo, D. (2017). Nutritional, physical and sensory properties of extruded products from high-amylose corn grits. *Emirates Journal of Food and Agriculture*, 846. https://doi.org/10.9755/ejfa.2017.v29.i11.1494

ltd, R. and M. (2025). *Extruded Snacks—Global Strategic Business Report*. Retrieved July 20, 2025, from https://www.researchandmarkets.com/reports/5302672/extruded-snacks-global-strategic-business-report

LUO, C. L. (2019). *Extruded Starch-Based Ready-to-Eat Snack and Methods of Making* (United States Patent No. US20190021374A1). https://patents.google.com/patent/US20190021374A1/en

Lyu, J. S., Lee, J.-S., Chae, T. Y., Yoon, C. S., & Han, J. (2023). Effect of screw speed and die temperature on physicochemical, textural, and morphological properties of soy protein isolate-based textured vegetable protein produced via a low-moisture extrusion. *Food Science and Biotechnology*, *32*(5), 659–669. https://doi.org/10.1007/s10068-022-01207-8

Maskus, H., & Arntfield, S. (2015). Extrusion processing and evaluation of an expanded, puffed pea snack product. *Journal of Nutrition & Food Sciences*, *5*(4), 1.

Mazumder, P., Roopa, B. S., & Bhattacharya, S. (2007). Textural attributes of a model snack food at different moisture contents. *Journal of Food Engineering*, *79*(2), 511–516. https://doi.org/10.1016/j.jfoodeng.2006.02.011

Mohammed, I., Forsido, S. F., & Kuyu, C. G. (2024). Optimization of barrel temperature and feed moisture content for better physicochemical and sensory properties of extruded snacks from blends of finger millet, sweet potato, and soybean composite flour using response surface methodology. *Discover Applied Sciences*, *6*(4). https://doi.org/10.1007/s42452-024-05822-4

Monfreda, C., Ramankutty, N., & Foley, J. A. (2008). Farming the planet: 2. Geographic distribution of crop areas, yields, physiological types, and net primary production in the year 2000. *Global Biogeochemical Cycles*, *22*(1). https://doi.org/10.1029/2007GB002947

Neder-Suárez, D., Amaya-Guerra, C. A., Pérez-Carrillo, E., Quintero-Ramos, A., Mendez-Zamora, G., Sánchez-Madrigal, M. Á., Barba-Dávila, B. A., & Lardizábal-Gutiérrez, D. (2020). Optimization of an Extrusion Cooking Process to Increase Formation of Resistant Starch from Corn Starch with Addition of Citric Acid. *Starch - Stärke*, *72*(3–4). https://doi.org/10.1002/star.201900150

Nor, N. M., Carr, A., Hardacre, A., & Brennan, C. S. (2013). The Development of Expanded Snack Product Made from Pumpkin Flour-Corn Grits: Effect of Extrusion Conditions and Formulations on Physical Characteristics and Microstructure. *Foods*, *2*(2), Article 2. https://doi.org/10.3390/foods2020160

Oke, M. O., Awonorin, S. O., & Workneh, T. S. (2013). Expansion ratio of extruded water yam (Dioscorea alata) starches using a single screw extruder. *African Journal of Agricultural Research*, *8*(9), 750–762.

Okunola, A. A., Dottie, E. P., Moses, O. I., Adekanye, T. A., Okonkwo, C. E., Kaveh, M., Szymanek, M., & Aremu, C. O. (2023). Development and Process Optimization of a Ready-to-Eat Snack from Rice-Cowpea Composite by a Twin Extruder. *Processes*, *11*(7), 2159. https://doi.org/10.3390/pr11072159

Philipp, C., Buckow, R., Silcock, P., & Oey, I. (2017). Instrumental and sensory properties of pea protein-fortified extruded rice snacks. *Food Research International*.

Pietsch, V. L., Werner, R., Karbstein, H. P., & Emin, M. A. (2019). High moisture extrusion of wheat gluten: Relationship between process parameters, protein polymerization, and final product characteristics. *Journal of Food Engineering*, *259*, 3–11. https://doi.org/10.1016/j.jfoodeng.2019.04.006

Pismag, R. Y., Rivera, J. D., Hoyos, J. L., Bravo, J. E., & Roa, D. F. (2024). Effect of extrusion cooking on physical and thermal properties of instant flours: A review. *Frontiers in Sustainable Food Systems*, *8*. https://doi.org/10.3389/fsufs.2024.1398908

Rangira, I., Gu, B., Ek, P., & Ganjyal, G. M. (2020). Pea starch exhibits good expansion characteristics under relatively lower temperatures during extrusion cooking. *Journal of Food Science*, *85*(10), 3333–3344. https://doi.org/10.1111/1750-3841.15450

Rani, P., Kumar, A., Purohit, S. R., & Rao, P. S. (2021). Extrusion of fermented rice-black gram flour for development of functional snacks: Characterization, optimization and sensory analysis. *Journal of Food Science and Technology*, *58*(2), 494–509. https://doi.org/10.1007/s13197-020-04558-4

Rusch, H. L., Hunter, M. C., Kraus, A., Tautges, N. E., & Jungers, J. M. (2025). Intermediate wheatgrass as a dual use crop for grain and grazing. *Frontiers in Agronomy*, *7*. https://doi.org/10.3389/fagro.2025.1534962

Sahu, C., Patel, S., & Tripathi, A. K. (2022). Effect of extrusion parameters on physical and functional quality of soy protein enriched maize based extruded snack. *Applied Food Research*, *2*(1), 100072. https://doi.org/10.1016/j.afres.2022.100072

Schendel, R. R., Becker, A., Tyl, C. E., & Bunzel, M. (2015). Isolation and characterization of feruloylated arabinoxylan oligosaccharides from the perennial cereal grain intermediate wheat grass (*Thinopyrum intermedium*). *Carbohydrate Research*, *407*, 16–25. https://doi.org/10.1016/j.carres.2015.01.006

Sharma, P., & Gujral, H. S. (2013). Extrusion of Hulled Barley Affecting β-Glucan and Properties of Extrudates. *Food and Bioprocess Technology*, *6*(6), 1374–1389. https://doi.org/10.1007/s11947-011-0777-2

Singh, B., Rachna, Hussain, S. Z., & Sharma, S. (2015). Response Surface Analysis and Process Optimization of Twin Screw Extrusion Cooking of Potato-Based Snacks: Extrusion Cooking of Potato-Based Snacks. *Journal of Food Processing and Preservation*, *39*(3), 270–281. https://doi.org/10.1111/jfpp.12230

Singh, R. K. R., Majumdar, R. K., & Venkateshwarlu, G. (2014). Effect of Process Conditions on Physico-Chemical and Sensory Properties of Fish-Cereal-Based Extruded Snack-Like Products. *Journal of Food Processing and Preservation*, *38*(1), 68–82. https://doi.org/10.1111/j.1745-4549.2012.00746.x

Singh, S., Gamlath, S., & Wakeling, L. (2007). Nutritional aspects of food extrusion: A review. *International Journal of Food Science and Technology*, *42*(8), 916–929. https://doi.org/10.1111/j.1365-2621.2006.01309.x

Singha, P., & Muthukumarappan, K. (2018). Single screw extrusion of apple pomace-enriched blends: Extrudate characteristics and determination of optimum processing conditions. *Food Science and Technology International*, *24*(5).

Srivastava, S., Genitha, T. R., & Yadav, V. (2012). Preparation and quality evaluation of flour and biscuit from sweet potato. *J Food Process Technol*, *3*(12), 1–5.

Sukumar, A., & Athmaselvi, K. A. (2019). Optimization of process parameters for the development of finger millet based multigrain extruded snack food fortified with banana powder using RSM. *Journal of Food Science and Technology*, *56*(2), 705–712. https://doi.org/10.1007/s13197-018-3527-x

Thingnes, S. L., Gaustad, A. H., Kjos, N. P., Hetland, H., & Framstad, T. (2013). Pea starch meal as a substitute for cereal grain in diets for lactating sows: The effect on sow and litter performance. *Livestock Science*, *157*(1), 210–217. https://doi.org/10.1016/j.livsci.2013.06.023

Tyl, C., & Ismail, B. P. (2019). Compositional evaluation of perennial wheatgrass (Thinopyrum intermedium) breeding populations. *International Journal of Food Science and Technology*, *54*(3), 660–669. https://doi.org/10.1111/ijfs.13925

Uribe-Wandurraga, Z. N., Igual, M., García-Segovia, P., & Martínez-Monzó, J. (2020). Influence of microalgae addition in formulation on colour, texture, and extrusion parameters of corn snacks. *Food Science and Technology International*, *26*(8), 685–695. https://doi.org/10.1177/1082013220924178

Van Hoan, N., Mouquet-Rivier, C., & Treche, S. (2010). Effects of Starch, Lipid and Moisture Contents on Extrusion Behavior and Extrudate Characteristics of Rice-Based Blends Prepared with a Very-Low-Cost Extruder. *Journal of Food Process Engineering*, *33*(3), 519–539. https://doi.org/10.1111/j.1745-4530.2008.00288.x

Wang, J., Xia, S., Wang, B., Ali, F., & Li, X. (2019). Effect of twin-screw extrusion on gelatinization characteristics of oat powder. *Journal of Food Process Engineering*, *42*(3). https://doi.org/10.1111/jfpe.13014

Wang, N., Maximiuk, L., & Toews, R. (2012). Pea starch noodles: Effect of processing variables on characteristics and optimisation of twin-screw extrusion process. *Food Chemistry*, *133*(3), 742–753. https://doi.org/10.1016/j.foodchem.2012.01.087

Wang, N., Warkentin, T. D., Vandenberg, B., & Bing, D. J. (2014). Physicochemical properties of starches from various pea and lentil varieties, and characteristics of their noodles prepared by high temperature extrusion. *Food Research International*, *55*, 119–127. https://doi.org/10.1016/j.foodres.2013.10.043

Ye, J., Hu, X., Luo, S., Liu, W., Chen, J., Zeng, Z., & Liu, C. (2018). Properties of Starch after Extrusion: A Review. *Starch - Stärke*, *70*(11–12). https://doi.org/10.1002/star.201700110

Zahari, I., Purhagen, J. K., Rayner, M., Ahlström, C., Helstad, A., Landers, M., Müller, J., Eriksson, J., & Östbring, K. (2023). Extrusion of high-moisture meat analogues from hempseed protein concentrate and oat fibre residue. *Journal of Food Engineering*, *354*, 111567. https://doi.org/10.1016/j.jfoodeng.2023.111567

Zhang, G., Ni, C., Ding, Y., Zhou, H., Caizhi, O., Wang, Q., Wang, J., & Cheng, J. (2020). Effects of Low Moisture Extrusion on the Structural and Physicochemical Properties of Adlay (Coix lacryma-jobi L.) Starch-Based Polymers. *Process Biochemistry*, *96*, 30–37. https://doi.org/10.1016/j.procbio.2020.05.028